UNIVERSIDAD DE CONCEPCIÓN

Centro de Investigación en Ingeniería Matemática (CI^{2}MA)

Pseudostress-based mixed finite element methods for the Stokes problem in R^n with Dirichlet boundary conditions. I: A priori error analysis

Gabriel N. Gatica, Antonio Marquez,
Manuel A. Sanchez

PREPRINT 2011-03

SERIE DE PRE-PUBLICACIONES

Pseudostress-based mixed finite element methods for the Stokes problem in $\mathbb{R}^n$ with Dirichlet boundary conditions. I: A priori error analysis

Gabriel N. Gatica[1,*], Antonio Márquez[2], Manuel A. Sánchez[1]

[1] *CI²MA and Departamento de Ingeniería Matemática, Universidad de Concepción, Casilla 160-C, Concepción, Chile*
[2] *Departamento de Construcción e Ingeniería de Fabricación, Universidad de Oviedo, Oviedo, España*

Abstract. We consider a non-standard mixed method for the Stokes problem in $\mathbb{R}^n$, $n \in \{2,3\}$, with Dirichlet boundary conditions, in which, after using the incompressibility condition to eliminate the pressure, the pseudostress tensor σ and the velocity vector $\mathbf{u}$ become the only unknowns. Then, we apply the Babuška-Brezzi theory to prove the well-posedness of the corresponding continuous and discrete formulations. In particular, we show that Raviart-Thomas elements of order $k \geq 0$ for σ and piecewise polynomials of degree k for $\mathbf{u}$ ensure unique solvability and stability of the associated Galerkin scheme. In addition, we introduce and analyze an augmented approach for our pseudostress-velocity formulation. The methodology employed is based on the introduction of the Galerkin least-squares type terms arising from the constitutive and equilibrium equations, and the Dirichlet boundary condition for the velocity, all of them multiplied by suitable stabilization parameters. We show that these parameters can be chosen so that the resulting augmented variational formulation is defined by a strongly coercive bilinear form, whence the associated Galerkin scheme becomes well posed for any choice of finite element subspaces. For instance, Raviart-Thomas elements of order $k \geq 0$ for σ and continuous piecewise polynomials of degree $k+1$ for $\mathbf{u}$ become a feasible choice in this case. Finally, extensive numerical experiments illustrating the good performance of the methods and comparing them with other procedures available in the literature, are provided.

AMS subject classifications: 65N15, 65N30, 65N50, 74B05
Key words: mixed finite element, pseudostress, incompressible flow.

1 Introduction

In the last decade there has been an increasing interest in new mixed finite element methods for linear and nonlinear Stokes problems. In particular, the velocity-pressure-stress

*Corresponding author. *Email addresses:* ggatica@ing-mat.udec.cl (G.N. Gatica), amarquez@uniovi.es (A. Márquez), manusanchez@udec.cl (M.A. Sánchez)

formulation and its natural applicability to non-Newtonian flows has gained notoriety in recent years. Among the main strengths of this and other related mixed formulations, we highlight the fact that, besides the original unknowns, they provide direct approximations of several other variables of physical interest. In addition, the stress-based formulations yield a unified analysis for linear and nonlinear flows. However, the increase in the number of degrees of freedom of the resulting discrete systems and the symmetry requirement for the stress tensor constitute the main drawbacks of the approaches involving this unknown. In order to circumvent these disadvantages two important ideas have already been suggested in the literature. The first one, which goes back to [15] and [1], consists of imposing the symmetry of the stress in a weak sense through the introduction of a suitable Lagrange multiplier (rotation in elasticity and vorticity in fluid mechanics). The second one, which is more appealing nowadays, is given by the use of the pseudostress tensor instead of the stress in the corresponding setting of the Stokes equations.

As a consequence of the latter idea mentioned above, two new approaches for incompressible flows, namely the velocity-pressure-pseudostress and velocity-pseudostress formulations, arised specially in the context of least-squares and augmented methods (see, e.g. [6], [8], [14]). In fact, augmented mixed finite element methods for both pseudostress-based formulations of the stationary Stokes equations, which extend the results derived for the Lamé system in [17], are introduced and analyzed in [14]. The corresponding augmented mixed finite element schemes for the stress-based formulations of the Stokes problem, in which the vorticity is introduced as the Lagrange multiplier taking care of the weak symmetry of the stress, had been previously studied in [13]. Other related methods for the steady Stokes problem, based on least-squares formulations with two or three fields among velocity, velocity gradient, pressure, vorticity, stress, and pseudostress, can be found in [3], [4], [7], [10], [11], and the references therein. Similarly, the extension of the results in [17] to the case of non-homogeneous Dirichlet boundary conditions in linear elasticity was provided in [16]. The use of the first Korn's inequality, as done in [17], is not possible in this case, and hence, an additional consistency term, determined precisely by the Dirichlet boundary condition, had to be incorporated into the augmented formulation. This extra term yielded the application of a modified Korn's inequality, which turned out to be crucial for the analysis in [16]. The results from [17] and [16] were extended in [19] to three-dimensional linear elasticity problems, while keeping the same advantages of the 2D case in the resulting augmented formulation.

Interestingly, the mixed finite element methods for the pure velocity-pseudotress formulation of the Stokes equations, that is without augmenting or employing least-squares terms, had not been studied in details until [9]. It is shown there that Raviart-Thomas elements of order $k \geq 0$ for the pseudostress and piecewise discontinuous polynomials of degree k for the velocity lead to a stable Galerkin scheme with quasi-optimal accuracy. The pressure and other physical quantities (if needed) can be computed via a post processing procedure without affecting the accuracy of approximation. In the recent paper [20] we reconsider the pure velocity-pseudostress formulation from [9] and pro-

vide further related results. More precisely, we incorporate the pressure unknown into the discrete analysis, which does not necessarily yield an equivalent formulation at that level, and derive reliable and efficient residual-based a posteriori error estimators for both Galerkin schemes. It is important to remark that the idea of reintroducing the pressure in [20] is to allow further flexibility in approximating this unknown. To this respect, we show there that a Galerkin scheme for the velocity-pressure-pseudostress formulation only makes sense for pressure finite element subspaces not containing the traces of the pseudostresses subspace. Otherwise, both discrete schemes coincide and hence one obviously stays with the simplest one. Furthermore, the extension of the results from [20] to a class of nonlinear problems, particularly those studied in [18] and [24], has been provided recently in [21]. Indeed, in [21] we develop the a priori and a posteriori error analyses of the velocity-pseudostress formulation as applied to quasi-Newtonian Stokes flows whose kinematic viscosities are a nonlinear monotone function of the velocity gradient of the fluid. The latter is introduced as an auxiliary unknown, and the pressure is eliminated using the incompressibility condition, whence the resulting variational formulation shows a twofold saddle point structure (as in [18] and [24]). In addition, an augmented version of this formulation, which, thanks to its single saddle point structure, simplifies the requirements for well-posedness of the associated Galerkin scheme, is also introduced and analyzed.

Now, in spite of the numerous contributions available in the literature concerning the application of pseudostress-based formulations in continuum mechanics, it is surprising to realize that most of them, except possibly [19], have to do with 2D boundary value problems. According to the above, the purpose of the present paper is to extend the results provided in [20] and [14] to the three-dimensional case. More precisely, in this first part we develop the a priori error analysis of the velocity-pseudostress formulation from [20] and its augmented version from [14] as applied to the Stokes problem in $\mathbb{R}^n$, $n \in \{2,3\}$. For simplicity we do not include the pressure unknown into our analysis since, similarly as observed in [20] and [14], the corresponding results arise from simple modifications of those obtained for the velocity-pseudostress formulations. In a subsequent paper we will address the corresponding a posteriori error analyses and the associated adaptive algorithms.

In order to describe the boundary value problem of interest, we now let Ω be a bounded and simply connected polyhedral domain in $\mathbb{R}^n$, $n \in \{2,3\}$, and boundary Γ. Our goal is to determine the velocity $\mathbf{u}$, the pseudostress tensor σ, and the pressure p of a steady flow occupying the region Ω, under the action of external forces. More precisely, given a volume force $\mathbf{f} \in [L^2(\Omega)]^n$ and $\mathbf{g} \in [H^{1/2}(\Gamma)]^n$, we seek a tensor field σ, a vector field $\mathbf{u}$, and a scalar field p such that

$$\begin{aligned} \sigma = 2\mu\nabla\mathbf{u} - p\mathbf{I} \quad \text{in} \quad \Omega, \qquad \mathbf{div}(\sigma) = -\mathbf{f} \quad \text{in} \quad \Omega, \\ \mathrm{div}(\mathbf{u}) = 0 \quad \text{in} \quad \Omega, \quad \mathbf{u} = \mathbf{g} \quad \text{on} \quad \Gamma, \end{aligned} \tag{1.1}$$

where μ is the kinematic viscosity and $\mathbf{div}$ stands for the usual divergence operator div

acting along each row of the tensor. As required by the incompressibility condition, we assume from now on that the datum $\mathbf{g}$ satisfies the compatibility condition

$$\int_\Gamma \mathbf{g}\cdot\boldsymbol{\nu} = 0, \tag{1.2}$$

where $\boldsymbol{\nu}$ stands for the unit outward normal at Γ. The rest of this work is organized as follows. In Section 2 we introduce the pseudostress-velocity approach and analyze the corresponding continuous and discrete formulations. In particular, we prove that Raviart-Thomas elements of order $k \geq 0$ for the pseudostress and piecewise polynomials of degree k for the velocity yield unique solvability and stability of the Galerkin scheme. Next, in Section 3 we consider an augmented version of the pseudostress-velocity approach, whose resulting variational formulation is defined by a strongly coercive bilinear form. As a consequence, the corresponding Galerkin scheme becomes well posed for any choice of finite element subspaces. Finally, several numerical results illustrating the good performance of our mixed finite element schemes and comparing them with other methods available in the literature, are provided in Section 4.

We end this section with several notations, some of them already employed above and other to be used below. Given any Hilbert space U, U^n and $U^{n\times n}$ denote, respectively, the space of vectors and square matrices of order n with entries in U. In addition, $\mathbf{I}$ is the identity matrix of $\mathbb{R}^{n\times n}$, and given $\boldsymbol{\tau} := (\tau_{ij})$, $\boldsymbol{\zeta} := (\zeta_{ij}) \in \mathbb{R}^{n\times n}$, we write as usual

$$\boldsymbol{\tau}^{\mathtt{t}} := (\tau_{ji}), \quad \mathrm{tr}(\boldsymbol{\tau}) := \sum_{i=1}^{n} \tau_{ii}, \quad \boldsymbol{\tau}^{\mathtt{d}} := \boldsymbol{\tau} - \frac{1}{n}\mathrm{tr}(\boldsymbol{\tau})\mathbf{I}, \quad \text{and} \quad \boldsymbol{\tau} : \boldsymbol{\zeta} := \sum_{i,j=1}^{n} \tau_{ij}\zeta_{ij}.$$

Also, in what follows we utilize the standard terminology for Sobolev spaces and norms, employ $\mathbf{0}$ to denote a generic null vector, and use C and c, with or without subscripts, bars, tildes or hats, to denote generic constants independent of the discretization parameters, which may take different values at different places.

2 The pseudostress-velocity approach

2.1 The continuous formulation

We begin by observing from the first equation in (1.1), using that $\mathrm{tr}(\nabla\mathbf{u}) = \mathrm{div}(\mathbf{u})$ in Ω, that the incompressibility condition $\mathrm{div}(\mathbf{u}) = 0 \quad \text{in} \quad \Omega$ can be stated in terms of the pseudostress tensor and the pressure as follows

$$p + \frac{1}{n}\mathrm{tr}(\boldsymbol{\sigma}) = 0 \quad \text{in} \quad \Omega. \tag{2.1}$$

Conversely, starting from (2.1), and using the first equation in (1.1), we recover the incompressibility condition $\mathrm{div}(\mathbf{u}) = 0 \quad \text{in} \quad \Omega$. In other words, the pair of equations given by

$$\boldsymbol{\sigma} = 2\mu\nabla\mathbf{u} - p\mathbf{I} \quad \text{in} \quad \Omega \quad \text{and} \quad \mathrm{div}(\mathbf{u}) = 0 \quad \text{in} \quad \Omega, \tag{2.2}$$

is equivalent to

$$\boldsymbol{\sigma} = 2\mu\nabla\mathbf{u} - p\mathbf{I} \quad \text{in} \quad \Omega \quad \text{and} \quad p + \frac{1}{n}\mathrm{tr}(\boldsymbol{\sigma}) = 0 \quad \text{in} \quad \Omega, \tag{2.3}$$

and therefore, instead of (1.1), we now consider:

$$\begin{aligned} \boldsymbol{\sigma} = 2\mu\nabla\mathbf{u} - p\mathbf{I} \quad \text{in} \quad \Omega, \qquad \mathbf{div}(\boldsymbol{\sigma}) = -\mathbf{f} \quad \text{in} \quad \Omega, \\ p + \frac{1}{n}\mathrm{tr}(\boldsymbol{\sigma}) = 0 \text{ in } \Omega, \quad \mathbf{u} = \mathbf{g} \quad \text{on} \quad \Gamma. \end{aligned} \tag{2.4}$$

Moreover, we proceed to eliminate the pressure, that is we replace p by $-\frac{1}{n}\mathrm{tr}(\boldsymbol{\sigma})$ in the first equation of the (2.4), which yields the following reduced problem with the pseudostress $\boldsymbol{\sigma}$ and the velocity $\mathbf{u}$ as the only unknowns:

$$\frac{1}{2\mu}\boldsymbol{\sigma}^{\mathrm{d}} = \nabla\mathbf{u} \quad \text{in} \quad \Omega, \qquad \mathbf{div}(\boldsymbol{\sigma}) = -\mathbf{f} \quad \text{in} \quad \Omega, \quad \mathbf{u} = \mathbf{g} \quad \text{on} \quad \Gamma. \tag{2.5}$$

Next, we adopt the usual procedure and test the two field equations of (2.5) with $\boldsymbol{\tau} \in H(\mathbf{div};\Omega)$ and $\mathbf{v} \in [L^2(\Omega)]^n$, respectively. In this way, noting that $\boldsymbol{\sigma}^{\mathrm{d}} : \boldsymbol{\tau} = \boldsymbol{\sigma}^{\mathrm{d}} : \boldsymbol{\tau}^{\mathrm{d}}$, integrating by parts the expression $\displaystyle\int_\Omega \nabla\mathbf{u} : \boldsymbol{\tau}$, and using the Dirichlet boundary condition, we arrive at the variational formulation: Find $(\boldsymbol{\sigma},\mathbf{u})$ in $H(\mathbf{div};\Omega) \times [L^2(\Omega)]^n$ such that

$$\begin{aligned} \frac{1}{2\mu}\int_\Omega \boldsymbol{\sigma}^{\mathrm{d}} : \boldsymbol{\tau}^{\mathrm{d}} + \int_\Omega \mathbf{u} \cdot \mathbf{div}(\boldsymbol{\tau}) = \langle \boldsymbol{\tau}\boldsymbol{\nu}, \mathbf{g} \rangle, \\ \int_\Omega \mathbf{v} \cdot \mathbf{div}(\boldsymbol{\sigma}) = -\int_\Omega \mathbf{f} \cdot \mathbf{v}, \end{aligned} \tag{2.6}$$

for all $(\boldsymbol{\tau},\mathbf{v}) \in H(\mathbf{div};\Omega) \times [L^2(\Omega)]^n$, where

$$H(\mathbf{div};\Omega) := \left\{ \boldsymbol{\tau} \in [L^2(\Omega)]^{n\times n} : \quad \mathbf{div}(\boldsymbol{\tau}) \in [L^2(\Omega)]^n \right\},$$

and $\langle \cdot,\cdot \rangle$ denotes the duality pairing between $[H^{-1/2}(\Gamma)]^n$ and $[H^{1/2}(\Gamma)]^n$, with respect to the $[L^2(\Gamma)]^n$-inner product.

The following lemma establishes the non-uniqueness of the problem (2.6) and hence the need of reformulating it to guarantee its unique solvability.

Lemma 2.1. *The set of solutions of the homogeneous version of* (2.6) *is given by*

$$\left\{ (c\mathbf{I},\mathbf{0}) : \quad c \in \mathbb{R} \right\}.$$

Proof. Let $(\boldsymbol{\sigma},\mathbf{u})$ in $H(\mathbf{div};\Omega) \times [L^2(\Omega)]^n$ such that

$$\begin{aligned} \frac{1}{2\mu}\int_\Omega \boldsymbol{\sigma}^{\mathrm{d}} : \boldsymbol{\tau}^{\mathrm{d}} + \int_\Omega \mathbf{u} \cdot \mathbf{div}(\boldsymbol{\tau}) = 0, \\ \int_\Omega \mathbf{v} \cdot \mathbf{div}(\boldsymbol{\sigma}) = 0, \end{aligned} \tag{2.7}$$

for all $(\boldsymbol{\tau},\mathbf{v}) \in H(\mathbf{div};\Omega)\times[L^2(\Omega)]^n$. It is clear from the second equation of (2.7) that $\mathbf{div}(\sigma)=\mathbf{0}$, and taking $\boldsymbol{\tau}=\sigma$ in the first equation of (2.7), we deduce that $\sigma^{\mathtt{d}}=\mathbf{0}$, which yields $\sigma=c\mathbf{I}$ with $c\in\mathbb{R}$. Finally, thanks to the surjectivity of the operator $\mathbf{div}:H(\mathbf{div};\Omega)\to[L^2(\Omega)]^n$, we conclude from the first equation of (2.7) that $\mathbf{u}=\mathbf{0}$ in Ω. In fact, it suffices to take $\boldsymbol{\tau}:=\nabla\mathbf{z}$, where $\mathbf{z}\in[H^1_0(\Omega)]^n$ is the unique solution of the Dirichlet problem: $\Delta\mathbf{z}=\mathbf{u}$ in Ω, $\mathbf{z}=\mathbf{0}$ on Γ. □

In order to handle this non-uniqueness, we consider the well known decomposition

$$H(\mathbf{div};\Omega)=H_0\oplus\mathbb{R}\mathbf{I}, \tag{2.8}$$

where

$$H_0:=\Big\{\boldsymbol{\tau}\in H(\mathbf{div};\Omega):\quad \int_\Omega \mathrm{tr}(\boldsymbol{\tau})=0\Big\},$$

and require from now on that σ belongs to H_0. Equivalently, we are just going to look for the H_0-component of the original pseudostress σ. The following lemma guarantees that the corresponding test space can also be restricted to H_0, which throughout the rest of the paper is endowed with $\|\cdot\|_{\mathbf{div},\Omega}$, the norm of $H(\mathbf{div};\Omega)$.

Lemma 2.2. *Any solution of* (2.6) *with* $\sigma\in H_0$ *is also solution of: Find* $(\sigma,\mathbf{u})\in H_0\times[L^2(\Omega)]^n$ *such that*

$$\begin{aligned}\frac{1}{2\mu}\int_\Omega \sigma^{\mathtt{d}}:\boldsymbol{\tau}^{\mathtt{d}}+\int_\Omega \mathbf{u}\cdot\mathbf{div}(\boldsymbol{\tau})&=\langle\boldsymbol{\tau}\nu,\mathbf{g}\rangle,\\ \int_\Omega \mathbf{v}\cdot\mathbf{div}(\sigma)&=-\int_\Omega \mathbf{f}\cdot\mathbf{v},\end{aligned} \tag{2.9}$$

for all $(\boldsymbol{\tau},\mathbf{v})\in H_0\times[L^2(\Omega)]^n$. *Conversely, any solution of* (2.9) *is also a solution of* (2.6).

Proof. It is immediate that any solution of (2.6) with $\sigma\in H_0$ is also a solution of (2.9). Conversely, let $(\sigma,\mathbf{u})$ be a solution of (2.9). Because of (2.8) it suffices to prove that $(\sigma,\mathbf{u})$ also satisfies (2.6) if tested with $(\mathbf{I},\mathbf{0})$, which can be seen to be true thanks to the compatibility condition (1.2). □

According to the previous lemma we now focus our analysis on problem (2.9). To this end, we first introduce the space $Q:=[L^2(\Omega)]^n$ and the bilinear forms $a:H_0\times H_0\longrightarrow\mathbb{R}$ and $b:H_0\times Q\to\mathbb{R}$ defined by

$$a(\boldsymbol{\zeta},\boldsymbol{\tau}):=\frac{1}{2\mu}\int_\Omega \boldsymbol{\zeta}^{\mathtt{d}}:\boldsymbol{\tau}^{\mathtt{d}}\qquad\forall(\boldsymbol{\zeta},\boldsymbol{\tau})\in H_0\times H_0, \tag{2.10}$$

and

$$b(\boldsymbol{\zeta},\mathbf{v}):=\int_\Omega \mathbf{v}\cdot\mathbf{div}(\boldsymbol{\zeta})\qquad\forall(\boldsymbol{\zeta},\mathbf{v})\in H_0\times Q. \tag{2.11}$$

Then, the variational formulation (2.9) can be rewritten as: Find $(\boldsymbol{\sigma},\mathbf{u}) \in H_0 \times Q$ such that

$$\begin{aligned} a(\boldsymbol{\sigma},\boldsymbol{\tau}) + b(\boldsymbol{\tau},\mathbf{u}) &= \langle \boldsymbol{\tau}\boldsymbol{\nu},\mathbf{g}\rangle \qquad \forall \boldsymbol{\tau} \in H_0, \\ b(\boldsymbol{\sigma},\mathbf{v}) &= -\int_\Omega \mathbf{f}\cdot\mathbf{v} \qquad \forall \mathbf{v} \in Q. \end{aligned} \tag{2.12}$$

The following well known estimate is needed to prove that (2.12) is well-posed.

Lemma 2.3. *There exists $c_1 > 0$, depending only on Ω, such that*

$$c_1 \|\boldsymbol{\tau}\|_{0,\Omega}^2 \leq \|\boldsymbol{\tau}^{\mathrm{d}}\|_{0,\Omega}^2 + \|\mathbf{div}(\boldsymbol{\tau})\|_{0,\Omega}^2 \quad \forall \boldsymbol{\tau} \in H_0. \tag{2.13}$$

Proof. See Lemma 3.1 in [2] or Proposition 3.1 of Chapter IV in [5]. □

Then we have the following main result.

Theorem 2.1. *Problem* (2.12) *has a unique solution $(\boldsymbol{\sigma},\mathbf{u}) \in H_0 \times Q$. Moreover, there exists a positive constant C, depending only on Ω, such that*

$$\|(\boldsymbol{\sigma},\mathbf{u})\|_{H_0\times Q} \leq C \left\{ \|\mathbf{f}\|_{0,\Omega} + \|\mathbf{g}\|_{1/2,\Gamma} \right\}.$$

Proof. It suffices to prove that the bilinear forms a and b satisfy the hypotheses of the Babuška-Brezzi theory. Indeed, given $\mathbf{v}$ in Q, we proceed as in the proof of Lemma 2.1 and let $\mathbf{z} \in [H_0^1(\Omega)]^n$ be the unique weak solution of the boundary value problem:

$$\Delta \mathbf{z} = \mathbf{v} \quad \text{in} \quad \Omega, \quad \mathbf{z} = \mathbf{0} \quad \text{on} \quad \Gamma. \tag{2.14}$$

Then, we let $\bar{\boldsymbol{\tau}} := \nabla \mathbf{z}$, note that $\bar{\boldsymbol{\tau}} \in H(\mathbf{div};\Omega)$, and decompose $\bar{\boldsymbol{\tau}} = \bar{\boldsymbol{\tau}}_0 + c_0\mathbf{I}$, with $\bar{\boldsymbol{\tau}}_0 \in H_0$ and $c_0 \in \mathbb{R}$. It follows that $\mathbf{div}(\bar{\boldsymbol{\tau}}_0) = \mathbf{div}(\bar{\boldsymbol{\tau}}) = \mathbf{v}$, which proves that the bounded linear operator $\mathbf{div}: H_0 \to [L^2(\Omega)]^n$ is surjective, as well. Equivalently, the bilinear form b satisfies the continuous inf-sup condition, which means that there exists $\beta > 0$ such that

$$\sup_{\substack{\boldsymbol{\tau}\in H_0 \\ \boldsymbol{\tau}\neq\mathbf{0}}} \frac{\displaystyle\int_\Omega \mathbf{v}\cdot\mathbf{div}(\boldsymbol{\tau})}{\|\boldsymbol{\tau}\|_{\mathbf{div},\Omega}} \geq \beta \|\mathbf{v}\|_{0,\Omega} \qquad \forall \mathbf{v} \in [L^2(\Omega)]^n. \tag{2.15}$$

Now, let V be the kernel of the operator induced by b, that is

$$V := \{\boldsymbol{\tau} \in H_0 : \quad b(\boldsymbol{\tau},\mathbf{v}) = 0 \quad \forall \mathbf{v} \in Q\} = \{\boldsymbol{\tau} \in H_0 : \quad \mathbf{div}(\boldsymbol{\tau}) = \mathbf{0}\}. \tag{2.16}$$

Then, applying Lemma 2.3, we find that for each $\boldsymbol{\tau} \in V$ there holds

$$a(\boldsymbol{\tau},\boldsymbol{\tau}) = \frac{1}{2\mu}\|\boldsymbol{\tau}^{\mathrm{d}}\|_{0,\Omega}^2 \geq \frac{c_1}{2\mu}\|\boldsymbol{\tau}\|_{0,\Omega}^2 = \frac{c_1}{2\mu}\|\boldsymbol{\tau}\|_{\mathbf{div},\Omega}^2, \tag{2.17}$$

which shows that the bilinear form a is strongly coercive in V. Finally, a direct application of Theorem 4.1 in Chapter I of [22] completes the proof. □

We end this section with the converse of the derivation of (2.12). More precisely, the following theorem establishes that the unique solution $(\boldsymbol{\sigma},\mathbf{u}) \in H_0 \times Q$ of (2.12) solves the original boundary value problem (2.5).

Theorem 2.2. *Let $(\boldsymbol{\sigma},\mathbf{u}) \in H_0 \times Q$ be the unique solution of* (2.12)*. Then, there hold in the distributional sense*

$$\frac{1}{2\mu}\boldsymbol{\sigma}^{\mathrm{d}} = \nabla \mathbf{u} \quad \textit{in} \quad \Omega, \qquad \mathbf{div}(\boldsymbol{\sigma}) = -\mathbf{f} \quad \textit{in} \quad \Omega, \quad \mathbf{u} = \mathbf{g} \quad \textit{on} \quad \Gamma,$$

which shows, in particular, that $\mathbf{u} \in [H^1(\Omega)]^n$.

Proof. It is clear from the second equation of (2.12) that $\mathbf{div}(\boldsymbol{\sigma}) = -\mathbf{f}$ in Ω. Next, we recall from Lemma 2.2 that the ocurrence of the first equation of (2.12) is equivalent to require it for each $\boldsymbol{\tau} \in H(\mathbf{div};\Omega)$. Hence, the other two identities follow by integrating backwardly the left hand side of this equation. We omit further details. □

2.2 The Galerkin scheme

Let $H^{\boldsymbol{\sigma}}_{0,h}$ and Q_h be arbitrary finite element subspaces of H_0 and Q, respectively. Then, the Galerkin scheme associated with (2.12) reads: Find $(\boldsymbol{\sigma}_h,\mathbf{u}_h) \in H^{\boldsymbol{\sigma}}_{0,h} \times Q_h$ such that

$$\begin{aligned} a(\boldsymbol{\sigma}_h,\boldsymbol{\tau}) + b(\boldsymbol{\tau},\mathbf{u}_h) &= \langle \boldsymbol{\tau}\boldsymbol{\nu},\mathbf{g}\rangle \qquad \forall \boldsymbol{\tau} \in H^{\boldsymbol{\sigma}}_{0,h}, \\ b(\boldsymbol{\sigma}_h,\mathbf{v}) &= -\int_\Omega \mathbf{f}\cdot\mathbf{v} \qquad \forall \mathbf{v} \in Q_h. \end{aligned} \tag{2.18}$$

In order to introduce explicit finite element subspaces guaranteeing the unique solvability and stability of (2.18), we now let $\{\mathcal{T}_h\}_{h>0}$ be a regular family of triangulations of the region $\bar{\Omega}$ by tetrahedrons T of diameter h_T such that $\bar{\Omega} = \cup\{T : T \in \mathcal{T}_h\}$ and define $h := \max\{h_T : T \in \mathcal{T}_h\}$. The faces of the tetrahedrons of $\mathcal{T}_h$ are denoted by e and their corresponding diameters by h_e. Certainly, we are assuming here that $n = 3$. In the case $n = 2$ we just need to replace tetrahedrons by triangles and faces by edges in what follows. Now, given an integer $\ell \geq 0$ and a subset S of $\mathbb{R}^n$, we denote by $\mathbb{P}_\ell(S)$ the space of polynomials of total degree at most ℓ defined on S. Then, for each integer $k \geq 0$ and for each $T \in \mathcal{T}_h$, we define the local Raviart-Thomas space of order k (see, e.g. [25], [5])

$$\mathbb{RT}_k(T) = [\mathbb{P}_k(T)]^n \oplus \mathbb{P}_k(T)\mathbf{x}, \tag{2.19}$$

where $\mathbf{x} := \begin{pmatrix} x_1 \\ \vdots \\ x_n \end{pmatrix}$ is a generic vector of $\mathbb{R}^n$, and let $\mathbb{RT}_k(\mathcal{T}_h)$ be the corresponding global space, that is

$$\mathbb{RT}_k(\mathcal{T}_h) := \big\{ \boldsymbol{\tau} \in H(\mathbf{div};\Omega) : \quad (\tau_{i1},\ldots,\tau_{in})^{\mathtt{t}} \in \mathbb{RT}_k(T) \quad \forall i \in \{1,\ldots,n\}, \quad \forall T \in \mathcal{T}_h \big\}. \tag{2.20}$$

We also let $\mathbb{P}_k(\mathcal{T}_h)$ be the global space of piecewise polynomials of degree $\leq k$, that is

$$\mathbb{P}_k(\mathcal{T}_h) := \big\{ v \in L^2(\Omega) : \quad v|_T \in \mathbb{P}_k(T) \quad \forall T \in \mathcal{T}_h \big\}. \tag{2.21}$$

Then we introduce the following finite element subspaces of H_0 and Q, respectively,

$$\begin{array}{rcl} H_{0,h}^{\sigma} & := & \Big\{ \boldsymbol{\tau} \in \mathbb{RT}_k(\mathcal{T}_h) : \quad \displaystyle\int_\Omega \mathrm{tr}(\boldsymbol{\tau}) = 0 \Big\}, \\ Q_h & := & [\mathbb{P}_k(\mathcal{T}_h)]^n. \end{array} \tag{2.22}$$

Next, we provide the main approximation properties of these subspaces. For this purpose, we first let $\mathcal{E}_h^k : [H^1(\Omega)]^{n\times n} \longrightarrow \mathbb{RT}_k(\mathcal{T}_h)$ be the usual equilibrium interpolation operator (see, e.g. [25], [5]), which, given $\boldsymbol{\tau} \in [H^1(\Omega)]^{n\times n}$, is characterized by the following identities:

$$\int_e \mathcal{E}_h^k(\boldsymbol{\tau})\boldsymbol{\nu}\cdot\mathbf{r} = \int_e \boldsymbol{\tau}\boldsymbol{\nu}\cdot\mathbf{r} \qquad \forall \,\text{face}\, e \in \mathcal{T}_h, \quad \forall\, \mathbf{r} \in [\mathbb{P}_k(e)]^n, \quad \text{when} \quad k \geq 0, \tag{2.23}$$

and

$$\int_T \mathcal{E}_h^k(\boldsymbol{\tau}) : \mathbf{r} = \int_T \boldsymbol{\tau} : \mathbf{r} \qquad \forall\, T \in \mathcal{T}_h, \quad \forall\, \mathbf{r} \in [\mathbb{P}_{k-1}(T)]^{n\times n}, \quad \text{when} \quad k \geq 1. \tag{2.24}$$

It is easy to show, using (2.23) and (2.24), that

$$\mathbf{div}(\mathcal{E}_h^k(\boldsymbol{\tau})) = \mathcal{P}_h^k(\mathbf{div}(\boldsymbol{\tau})), \tag{2.25}$$

where $\mathcal{P}_h^k$ is the orthogonal projector from $[L^2(\Omega)]^n$ into $[\mathbb{P}_k(\mathcal{T}_h)]^n$. In addition, it is well known (see, e.g. [12]) that for each $\mathbf{v} \in [H^m(\Omega)]^n$, with $0 \leq m \leq k+1$, there holds

$$\|\mathbf{v} - \mathcal{P}_h^k(\mathbf{v})\|_{0,T} \leq C h_T^m |\mathbf{v}|_{m,T} \qquad \forall\, T \in \mathcal{T}_h. \tag{2.26}$$

Furthermore, the operator $\mathcal{E}_h^k$ satisfies the following estimates (see, e.g. [5], [25]):

$$\|\boldsymbol{\tau} - \mathcal{E}_h^k(\boldsymbol{\tau})\|_{0,T} \leq C h_T^m |\boldsymbol{\tau}|_{m,T} \qquad \forall\, T \in \mathcal{T}_h, \tag{2.27}$$

for each $\boldsymbol{\tau} \in [H^m(\Omega)]^{n\times n}$, with $1 \leq m \leq k+1$,

$$\|\mathbf{div}(\boldsymbol{\tau} - \mathcal{E}_h^k(\boldsymbol{\tau}))\|_{0,T} \leq C h_T^m |\mathbf{div}(\boldsymbol{\tau})|_{m,T} \qquad \forall\, T \in \mathcal{T}_h, \tag{2.28}$$

for each $\boldsymbol{\tau} \in [H^1(\Omega)]^{n\times n}$ such that $\mathbf{div}(\boldsymbol{\tau}) \in [H^m(\Omega)]^n$, with $0 \leq m \leq k+1$, and

$$\|\boldsymbol{\tau}\boldsymbol{\nu} - \mathcal{E}_h^k(\boldsymbol{\tau})\boldsymbol{\nu}\|_{0,e} \leq C h_e^{1/2} \|\boldsymbol{\tau}\|_{1,T_e} \qquad \forall \,\text{face}\, e \in \mathcal{T}_h, \tag{2.29}$$

for each $\boldsymbol{\tau} \in [H^1(\Omega)]^{n\times n}$, where T_e is any tetrahedron of $\mathcal{T}_h$ having e as a face. In particular, note that (2.28) follows easily from (2.25) and (2.26). Moreover, it turns out (see, e.g. Theorem 3.16 in [23]) that $\mathcal{E}_h^k$ can also be defined as a bounded linear operator from the

larger space $[H^s(\Omega)]^{n\times n}\cap H(\mathbf{div};\Omega)$ into $\mathbb{RT}_k(\mathcal{T}_h)$ for all $s\in(0,1]$, and that in this case there holds the following interpolation error estimate

$$\|\boldsymbol{\tau}-\mathcal{E}_h^k(\boldsymbol{\tau})\|_{0,T}\leq Ch_T^s\left\{\|\boldsymbol{\tau}\|_{s,T}+\|\mathbf{div}(\boldsymbol{\tau})\|_{0,T}\right\}\qquad\forall T\in\mathcal{T}_h. \tag{2.30}$$

Then, as a consequence of (2.26), (2.27), (2.28), (2.30), and the usual interpolation estimates, we find that the subspaces $H^{\sigma}_{0,h}$ and Q_h given by (2.22) satisfy the following approximation properties:

$(\mathrm{AP}^{\sigma}_{0,h})$ *For each* $s\in(0,k+1]$ *and for each* $\boldsymbol{\tau}\in[H^s(\Omega)]^{n\times n}\cap H_0$ *with* $\mathbf{div}(\boldsymbol{\tau})\in[H^s(\Omega)]^n$ *there exists* $\boldsymbol{\tau}_h\in H^{\sigma}_{0,h}$ *such that*

$$\|\boldsymbol{\tau}-\boldsymbol{\tau}_h\|_{\mathbf{div},\Omega}\leq Ch^s\left\{\|\boldsymbol{\tau}\|_{s,\Omega}+\|\mathbf{div}(\boldsymbol{\tau})\|_{s,\Omega}\right\}.$$

$(\mathrm{AP}^{\mathbf{u}}_{h})$ *For each* $s\in[0,k+1]$ *and for each* $\mathbf{v}\in[H^s(\Omega)]^n$ *there exists* $\mathbf{v}_h\in Q_h$ *such that*

$$\|\mathbf{v}-\mathbf{v}_h\|_{0,\Omega}\leq Ch^s\|\mathbf{v}\|_{s,\Omega}.$$

Having provided the above, we now establish the unique solvability, stability, and convergence of the Galerkin scheme (2.18) with the finite element subspaces given by (2.22). We begin the analysis with the discrete inf-sup condition for the bilinear form b.

Lemma 2.4. *Let* $H^{\sigma}_{0,h}$ *and* Q_h *be given by* (2.22)*. Then, there exists* $\beta>0$*, independent of* h*, such that*

$$\sup_{\substack{\boldsymbol{\tau}\in H^{\sigma}_{0,h}\\ \boldsymbol{\tau}\neq\mathbf{0}}}\frac{b(\boldsymbol{\tau},\mathbf{v})}{\|\boldsymbol{\tau}\|_{\mathbf{div},\Omega}}\geq\beta\|\mathbf{v}\|_{0,\Omega}\qquad\forall\mathbf{v}\in Q_h. \tag{2.31}$$

Proof. Since b satisfies the continuous inf-sup condition (cf. (2.15) in the proof of Theorem 2.1), we just need to construct a Fortin operator $\Pi_h:H_0\longrightarrow H^{\sigma}_{0,h}$. To this end, we first let G be a bounded convex polyhedral domain containing $\bar{\Omega}$. Then, given $\boldsymbol{\tau}\in H_0$, we let $\mathbf{z}\in[H^1_0(G)]^n$ be the unique weak solution of the boundary value problem:

$$\Delta\mathbf{z}=\left\{\begin{array}{lll}\mathrm{div}\,\boldsymbol{\tau} & \text{in} & \Omega\\ \mathbf{0} & \text{in} & G\backslash\Omega\end{array}\right.,\qquad\mathbf{z}=\mathbf{0}\quad\text{on}\quad\partial G. \tag{2.32}$$

Thanks to the elliptic regularity result for (2.32) we have that $\mathbf{z}\in[H^2(G)]^n$ and

$$\|\mathbf{z}\|_{2,G}\leq c\|\mathbf{div}(\boldsymbol{\tau})\|_{0,\Omega}. \tag{2.33}$$

Also, it is clear that $\nabla\mathbf{z}|_{\Omega}\in[H^1(\Omega)]^{n\times n}$, $\mathbf{div}(\nabla\mathbf{z})=\Delta\mathbf{z}=\mathbf{div}(\boldsymbol{\tau})$ in Ω, and

$$\|\nabla\mathbf{z}\|_{1,\Omega}\leq\|\mathbf{z}\|_{2,\Omega}\leq\|\mathbf{z}\|_{2,G}\leq c\,\|\mathbf{div}(\boldsymbol{\tau})\|_{0,\Omega}. \tag{2.34}$$

According to the above, we define $\Pi_h(\boldsymbol{\tau})$ as the H_0-component of $\mathcal{E}_h^k(\nabla \mathbf{z})$ determined by the decomposition (2.8), that is

$$\Pi_h(\boldsymbol{\tau}) := \mathcal{E}_h^k(\nabla \mathbf{z}) - \left\{ \frac{1}{n|\Omega|} \int_\Omega \mathrm{tr}(\mathcal{E}_h^k(\nabla \mathbf{z})) \right\} \mathbf{I}.$$

It follows, using (2.25), that

$$\mathbf{div}(\Pi_h(\boldsymbol{\tau})) = \mathbf{div}(\mathcal{E}_h^k(\nabla \mathbf{z})) = \mathcal{P}_h^k(\mathbf{div}(\nabla \mathbf{z})) = \mathcal{P}_h^k(\mathbf{div}(\boldsymbol{\tau})) \quad \text{in} \quad \Omega,$$

and hence for each $\mathbf{v} \in Q_h = [\mathbb{P}_k(\mathcal{T}_h)]^n$ there holds

$$b(\Pi_h(\boldsymbol{\tau}),\mathbf{v}) = \int_\Omega \mathbf{v}\cdot\mathbf{div}(\Pi_h(\boldsymbol{\tau})) = \int_\Omega \mathbf{v}\cdot\mathcal{P}_h^k(\mathbf{div}(\boldsymbol{\tau})) = \int_\Omega \mathbf{v}\cdot\mathbf{div}(\boldsymbol{\tau}) = b(\boldsymbol{\tau},\mathbf{v}). \tag{2.35}$$

In addition, using the stability of the decomposition (2.8), and applying (2.27) (with m=1) and (2.34), we find that

$$\|\Pi_h(\boldsymbol{\tau})\|^2_{\mathbf{div},\Omega} \leq \|\mathcal{E}_h^k(\nabla \mathbf{z})\|^2_{\mathbf{div},\Omega} = \|\mathcal{E}_h^k(\nabla \mathbf{z})\|^2_{0,\Omega} + \|\mathcal{P}_h^k(\mathbf{div}(\boldsymbol{\tau}))\|^2_{0,\Omega}$$
$$\leq C\left\{ \|\nabla \mathbf{z} - \mathcal{E}_h^k(\nabla \mathbf{z})\|^2_{0,\Omega} + \|\nabla \mathbf{z}\|^2_{0,\Omega} + \|\mathbf{div}(\boldsymbol{\tau})\|^2_{0,\Omega} \right\} \leq C\,\|\mathbf{div}(\boldsymbol{\tau})\|^2_{0,\Omega},$$

which shows that Π_h is uniformly bounded. The above estimate and (2.35) prove that Π_h becomes a Fortin operator, which finishes the proof. □

We are now in a position to establish the following theorems.

Theorem 2.3. *Let $H^\sigma_{0,h}$ and Q_h be given by* (2.22)*. Then the Galerkin scheme* (2.18) *has a unique solution $(\boldsymbol{\sigma}_h,\mathbf{u}_h) \in H^\sigma_{0,h} \times Q_h$, and there exist positive constants C, $\tilde{C}$, independent of h, such that*

$$\|(\boldsymbol{\sigma}_h,\mathbf{u}_h)\|_{H_0\times Q} \leq C\left\{ \|\mathbf{f}\|_{0,\Omega} + \|\mathbf{g}\|_{1/2,\Gamma} \right\},$$

and

$$\|(\boldsymbol{\sigma},\mathbf{u}) - (\boldsymbol{\sigma}_h,\mathbf{u}_h)\|_{H_0\times Q} \leq \tilde{C} \inf_{(\boldsymbol{\tau}_h,\mathbf{v}_h)\in H^\sigma_{0,h}\times Q_h} \|(\boldsymbol{\sigma},\mathbf{u}) - (\boldsymbol{\tau}_h,\mathbf{v}_h)\|_{H_0\times Q}. \tag{2.36}$$

Proof. Since $\mathrm{div}(H^\sigma_{0,h}) \subseteq Q_h$, we find that the discrete kernel of b is given by

$$V_h := \left\{ \boldsymbol{\tau} \in H^\sigma_{0,h} : \quad b(\boldsymbol{\tau},\mathbf{v}) = 0 \quad \forall \mathbf{v} \in Q_h \right\} = \left\{ \boldsymbol{\tau} \in H^\sigma_{0,h} : \quad \mathbf{div}(\boldsymbol{\tau}) = 0 \quad \text{in} \quad \Omega \right\},$$

which is clearly contained in V (cf. (2.16)), the continuous kernel of b, and hence, thanks to (2.17), a is strongly coercive in V_h as well. This fact, Lemma 2.4, and a direct application of the classical Babuška-Brezzi theory (see, e.g. Theorem 1.1 in Chapter II of [22]) complete the proof. □

Theorem 2.4. *Let $H^{\sigma}_{0,h}$ and Q_h be given by* (2.22) *and let $(\boldsymbol{\sigma},\mathbf{u})\in H_0\times Q$ and $(\boldsymbol{\sigma}_h,\mathbf{u}_h)\in H^{\sigma}_{0,h}\times Q_h$ be the unique solutions of the continuous and discrete formulations* (2.12) *and* (2.18)*, respectively. Assume that $\boldsymbol{\sigma}\in[H^s(\Omega)]^{n\times n}$, $\mathbf{div}(\boldsymbol{\sigma})\in[H^s(\Omega)]^n$, and $\mathbf{u}\in[H^s(\Omega)]^n$, for some $s\in(0,k+1]$. Then there exists $C>0$, independent of h, such that*

$$\|(\boldsymbol{\sigma},\mathbf{u})-(\boldsymbol{\sigma}_h,\mathbf{u}_h)\|_{H_0\times Q}\leq Ch^s\left\{\|\boldsymbol{\sigma}\|_{s,\Omega}+\|\mathbf{div}(\boldsymbol{\sigma})\|_{s,\Omega}+\|\mathbf{u}\|_{s,\Omega}\right\}.$$

Proof. It follows from the Cea estimate (2.36) and the approximation properties $(\mathrm{AP}^{\sigma}_{0,h})$ and $(\mathrm{AP}^{\mathbf{u}}_{h})$. □

3 The augmented pseudostress-velocity approach

In this section we extend the results from [14] to the three-dimensional case.

3.1 The continuous formulation

We begin by enriching the formulation (2.12) with residuals arising from the modified constitutive equation, the equilibrium equation, and the Dirichlet boundary condition (all of them displayed respectively in (2.5)). More precisely, following the same procedure from [17], [16] and [14], we subtract the second from the first equation in (2.12) and then add the Galerkin least-squares terms given by

$$\kappa_1\int_{\Omega}\left(\nabla\mathbf{u}-\frac{1}{2\mu}\boldsymbol{\sigma}^{\mathrm{d}}\right):\left(\nabla\mathbf{v}+\frac{1}{2\mu}\boldsymbol{\tau}^{\mathrm{d}}\right)=0, \tag{3.1}$$

$$\kappa_2\int_{\Omega}\mathbf{div}(\boldsymbol{\sigma})\cdot\mathbf{div}(\boldsymbol{\tau})=-\kappa_2\int_{\Omega}\mathbf{f}\cdot\mathbf{div}(\boldsymbol{\tau}), \tag{3.2}$$

and

$$\kappa_3\int_{\Gamma}\mathbf{u}\cdot\mathbf{v}=\kappa_3\int_{\Gamma}\mathbf{g}\cdot\mathbf{v}, \tag{3.3}$$

for all $(\boldsymbol{\tau},\mathbf{v})\in H_0\times[H^1(\Omega)]^n$, where $(\kappa_1,\kappa_2,\kappa_3)$ is a vector of positive parameters to be specified later. We notice that (3.1) and (3.3) implicitly require now the velocity $\mathbf{u}$ to live in the smaller space $[H^1(\Omega)]^n$ instead of $[L^2(\Omega)]^n$.

Thus, we propose to replace (2.12) by the following augmented variational formulation: Find $(\boldsymbol{\sigma},\mathbf{u})\in\boldsymbol{H}_0=H_0\times[H^1(\Omega)]^n$ such that

$$A((\boldsymbol{\sigma},\mathbf{u}),(\boldsymbol{\tau},\mathbf{v}))=F(\boldsymbol{\tau},\mathbf{v})\qquad\forall(\boldsymbol{\tau},\mathbf{v})\in\boldsymbol{H}_0, \tag{3.4}$$

where the bilinear form $A : \boldsymbol{H}_0 \times \boldsymbol{H}_0 \to \mathbb{R}$ and the functional $F : \boldsymbol{H}_0 \to \mathbb{R}$ are defined by

$$\begin{aligned} A((\boldsymbol{\zeta},\mathbf{w}),(\boldsymbol{\tau},\mathbf{v})) &:= a(\boldsymbol{\zeta},\boldsymbol{\tau}) + b(\boldsymbol{\tau},\mathbf{w}) - b(\boldsymbol{\zeta},\mathbf{v}) \\ &+ \quad \kappa_1 \int_\Omega \left(\nabla \mathbf{w} - \frac{1}{2\mu} \boldsymbol{\zeta}^{\mathrm{d}} \right) : \left(\nabla \mathbf{v} + \frac{1}{2\mu} \boldsymbol{\tau}^{\mathrm{d}} \right) \\ &+ \quad \kappa_2 \int_\Omega \mathbf{div}(\boldsymbol{\zeta}) \cdot \mathbf{div}(\boldsymbol{\tau}) + \kappa_3 \int_\Gamma \mathbf{w} \cdot \mathbf{v} \end{aligned} \tag{3.5}$$

and

$$F(\boldsymbol{\tau},\mathbf{v}) := \int_\Omega \mathbf{f} \cdot (\mathbf{v} - \kappa_2 \mathbf{div}(\boldsymbol{\tau})) + \langle \boldsymbol{\tau}\nu, \mathbf{g} \rangle + \kappa_3 \int_\Gamma \mathbf{g} \cdot \mathbf{v}, \tag{3.6}$$

for all $(\boldsymbol{\zeta},\mathbf{w}), (\boldsymbol{\tau},\mathbf{v}) \in \boldsymbol{H}_0$.

In what follows we aim to show the well-posedness of (3.4). The main idea is to choose the vector of parameters $(\kappa_1,\kappa_2,\kappa_3)$ in such a way that A becomes strongly coercive in $\boldsymbol{H}_0$ with respect to the norm $\|\cdot\|_{\boldsymbol{H}_0}$ defined by

$$\|(\boldsymbol{\tau},\mathbf{v})\|_{\boldsymbol{H}_0} := \left\{ \|\boldsymbol{\tau}\|^2_{\mathbf{div},\Omega} + \|\mathbf{v}\|^2_{1,\Omega} \right\}^{1/2} \qquad \forall (\boldsymbol{\tau},\mathbf{v}) \in \boldsymbol{H}_0, \tag{3.7}$$

and then to simply apply the classical Lax-Milgram Lemma. Indeed, we first observe that

$$\int_\Omega \left(\nabla \mathbf{v} - \frac{1}{2\mu} \boldsymbol{\tau}^{\mathrm{d}} \right) : \left(\nabla \mathbf{v} + \frac{1}{2\mu} \boldsymbol{\tau}^{\mathrm{d}} \right) = |\mathbf{v}|^2_{1,\Omega} - \frac{1}{4\mu^2} \|\boldsymbol{\tau}^{\mathrm{d}}\|^2_{0,\Omega}, \tag{3.8}$$

and hence, according to the definitions of a and A (cf. (2.10) and (3.5)), we find that

$$A((\boldsymbol{\tau},\mathbf{v}),(\boldsymbol{\tau},\mathbf{v})) = \frac{1}{2\mu} \left(1 - \frac{\kappa_1}{2\mu} \right) \|\boldsymbol{\tau}^{\mathrm{d}}\|^2_{0,\Omega} + \kappa_2 \|\mathbf{div}(\boldsymbol{\tau})\|^2_{0,\Omega} + \kappa_1 |\mathbf{v}|^2_{1,\Omega} + \kappa_3 \|\mathbf{v}\|^2_{0,\Gamma} \tag{3.9}$$

for each $(\boldsymbol{\tau},\mathbf{v}) \in \boldsymbol{H}_0$. Then, choosing κ_1, κ_2 and κ_3 such that $0 < \kappa_1 < 2\mu$ and $0 < \kappa_2, \kappa_3$, and applying Lemma 2.3, we deduce that

$$\begin{aligned} A((\boldsymbol{\tau},\mathbf{v}),(\boldsymbol{\tau},\mathbf{v})) &\geq \alpha_1 \left\{ \|\boldsymbol{\tau}^{\mathrm{d}}\|^2_{0,\Omega} + \|\mathbf{div}(\boldsymbol{\tau})\|^2_{0,\Omega} \right\} + \frac{\kappa_2}{2} \|\mathbf{div}(\boldsymbol{\tau})\|^2_{0,\Omega} + \alpha_2 \left\{ |\mathbf{v}|^2_{1,\Omega} + \|\mathbf{v}\|^2_{0,\Gamma} \right\} \\ &\geq c_1 \alpha_1 \|\boldsymbol{\tau}\|^2_{0,\Omega} + \frac{\kappa_2}{2} \|\mathbf{div}(\boldsymbol{\tau})\|^2_{0,\Omega} + \alpha_2 \left\{ |\mathbf{v}|^2_{1,\Omega} + \|\mathbf{v}\|^2_{0,\Gamma} \right\} \\ &\geq \alpha_3 \|\boldsymbol{\tau}\|^2_{\mathbf{div},\Omega} + \alpha_2 \left\{ |\mathbf{v}|^2_{1,\Omega} + \|\mathbf{v}\|^2_{0,\Gamma} \right\} \qquad \forall (\boldsymbol{\tau},\mathbf{v}) \in \boldsymbol{H}_0, \end{aligned}$$

where c_1 is the constant from Lemma 2.3,

$$\alpha_1 := \min \left\{ \frac{1}{2\mu} \left(1 - \frac{\kappa_1}{2\mu} \right), \frac{\kappa_2}{2} \right\}, \quad \alpha_2 := \min\{\kappa_1,\kappa_3\}, \quad \text{and} \quad \alpha_3 := \min \left\{ c_1\alpha_1, \frac{\kappa_2}{2} \right\}. \tag{3.10}$$

In order to complete the required estimate for A we need the following Korn type inequality.

Lemma 3.1. *There exists $c_2 > 0$, depending only on Ω, such that*

$$c_2 \|\mathbf{v}\|^2_{1,\Omega} \leq |\mathbf{v}|^2_{1,\Omega} + \|\mathbf{v}\|^2_{0,\Gamma} \qquad \forall \mathbf{v} \in [H^1(\Omega)]^n. \tag{3.11}$$

Proof. It suffices to apply the Peetre-Tartar Lemma (cf. [22, Theorem 2.1, Chapter I]) and the generalized Poincaré inequality. We omit further details and refer to [16, Section 3] for the proof of a similar estimate. □

It follows from the previous inequality satisfied by A and Lemma 3.1 that

$$A((\boldsymbol{\tau},\mathbf{v})) \geq \alpha \|(\boldsymbol{\tau},\mathbf{v})\|^2_{\boldsymbol{H}_0} \quad \forall (\boldsymbol{\tau},\mathbf{v}) \in \boldsymbol{H}_0, \tag{3.12}$$

where $\alpha := \min\{\alpha_3, c_2\alpha_2\}$, which confirms the strong coerciveness of A.

As a consequence of the above analysis we can establish the following main result.

Theorem 3.1. *Assume that there hold $0 < \kappa_1 < 2\mu$ and $0 < \kappa_2, \kappa_3$. Then, the augmented variational formulation* (3.4) *has a unique solution $(\boldsymbol{\sigma},\mathbf{u}) \in \boldsymbol{H}_0$, which coincides with the unique solution of* (2.12)*. Moreover, there exists a positive constant C, depending only on μ and $(\kappa_1,\kappa_2,\kappa_3)$, such that*

$$\|(\boldsymbol{\sigma},\mathbf{u})\|_{\boldsymbol{H}_0} \leq C \|F\|_{\boldsymbol{H}_0'} \leq C\{\|\mathbf{f}\|_{0,\Omega} + \|\mathbf{g}\|_{1/2,\Gamma}\}. \tag{3.13}$$

Proof. It is clear from (3.5) and (3.12) that A is bounded and strongly coercive on $\boldsymbol{H}_0$ with constants depending only on μ and $(\kappa_1,\kappa_2,\kappa_3)$. In addition, the Cauchy-Schwarz inequality in $[L^2(\Omega)]^n$ and $[L^2(\Gamma)]^n$, and the trace inequalities in $H(\mathbf{div};\Omega)$ and $[H^1(\Omega)]^n$ imply that the linear functional F (cf. (3.6)) is also bounded. Therefore, thanks to the Lax-Milgram Lemma, we deduce the existence of a unique $(\boldsymbol{\sigma},\mathbf{u}) \in \boldsymbol{H}_0$ solution to (3.4), which satisfies the stability estimate (3.13). Furthermore, it follows from Theorem 2.2 that the unique solution of (2.12) is also a solution of (3.4), and hence the solutions of both problems coincide. □

We end this section by remarking that the introduction of the equation (3.3) in the augmented formulation (3.4) is crucial to obtain, thanks to the inequality (3.11) (cf. Lemma 3.1), the term $\|\mathbf{v}\|^2_{1,\Omega}$ in the estimate (3.12). However, when the Dirichlet boundary condition is homogeneous, that is $\mathbf{g} = \mathbf{0}$, the equation (3.3) and the inequality (3.11) are not necessary since in this case the unknown $\mathbf{u}$ would live in $[H^1_0(\Omega)]^n$, space where the usual norm and semi-norm of $[H^1(\Omega)]^n$ are equivalent.

3.2 The Galerkin scheme

We now let $H^{\boldsymbol{\sigma}}_{0,h}$ and $H^{\mathbf{u}}_h$ be arbitrary finite element subspaces of H_0 and $[H^1(\Omega)]^n$, respectively, and define $\boldsymbol{H}_{0,h} := H^{\boldsymbol{\sigma}}_{0,h} \times H^{\mathbf{u}}_h$. Then, the Galerkin scheme associated with (3.4) reads: Find $(\boldsymbol{\sigma}_h,\mathbf{u}_h) \in \boldsymbol{H}_{0,h}$ such that

$$A((\boldsymbol{\sigma}_h,\mathbf{u}_h),(\boldsymbol{\tau},\mathbf{v})) = F(\boldsymbol{\tau},\mathbf{v}) \qquad \forall (\boldsymbol{\tau},\mathbf{v}) \in \boldsymbol{H}_{0,h}. \tag{3.14}$$

Since the bilinear form A is strongly coercive on any finite element subspace $\boldsymbol{H}_{0,h}$ of $\boldsymbol{H}_0$, the analogue of Theorem 2.3 for the augmented scheme (3.14) is easily established as follows.

Theorem 3.2. *Assume that the parameters κ_1,κ_2 and κ_3 satisfy the same assumptions of Theorem* 3.1*, and let $\boldsymbol{H}_{0,h}$ be any finite element subspace of $\boldsymbol{H}_0$. Then, the Galerkin scheme* (3.14) *has a unique solution $(\boldsymbol{\sigma}_h,\mathbf{u}_h)\in\boldsymbol{H}_{0,h}$, and there exist positive constants $C,\tilde{C}$, independent of h, such that*

$$\|(\boldsymbol{\sigma}_h,\mathbf{u}_h)\|_{\boldsymbol{H}_0}\leq C\Big\{\|\mathbf{f}\|_{0,\Omega}+\|\mathbf{g}\|_{1/2,\Gamma}\Big\},$$

and

$$\|(\boldsymbol{\sigma},\mathbf{u})-(\boldsymbol{\sigma}_h,\mathbf{u}_h)\|_{\boldsymbol{H}_0}\leq\tilde{C}\inf_{(\boldsymbol{\tau}_h,\mathbf{v}_h)\in\boldsymbol{H}_{0,h}}\|(\boldsymbol{\sigma},\mathbf{u})-(\boldsymbol{\tau}_h,\mathbf{v}_h)\|_{\boldsymbol{H}_0}. \tag{3.15}$$

Proof. It follows from a straightforward application of the Lax-Milgram Lemma and the corresponding Cea estimate. □

At this point we find it important to make a remark concerning the choice of the vector of parameters $(\kappa_1,\kappa_2,\kappa_3)$. In fact, besides the assumptions in Theorem 3.1, we may adopt as a criterion the maximization of the coerciveness constant α (cf. (3.12)). However, since the constants c_1 and c_2 from Lemmas 2.3 and 3.1 are not known explicitly, we simply aim to partially satisfy this goal. In this way, we can at least maximize the values of α_1 and α_2 (cf. (3.10)) by choosing, respectively,

$$\kappa_2=\frac{1}{\mu}\left(1-\frac{\kappa_1}{2\mu}\right)\qquad\text{and}\qquad\kappa_3=\kappa_1. \tag{3.16}$$

In particular, $\kappa_1=\mu$, which obviously satisfies the assumption $\kappa_1\in(0,2\mu)$, yields $\kappa_2=\dfrac{1}{2\mu}$ and $\kappa_3=\mu$. This constitutes precisely the vector of parameters utilized in the numerical examples shown below in Section 4. However, any other choice of $\kappa_1\in(0,2\mu)$ combined with (3.16) would certainly lead to a feasible set of parameters.

Now, in order to provide the rate of convergence of the augmented scheme (3.14) we need to consider a specific finite element subspace $\boldsymbol{H}_{0,h}$. Indeed, with the same notations and definitions from Section 2.2, and given an integer $k\geq 0$, we now let $H^{\boldsymbol{\sigma}}_{0,h}$ be the finite element subspace defined in (2.22), and introduce the usual Lagrange finite element subspace of $[H^1(\Omega)]^n$:

$$H^{\mathbf{u}}_h:=\Big\{\mathbf{v}_h\in[C(\bar{\Omega})]^n:\quad\mathbf{v}_h|_T\in[\mathbb{P}_{k+1}(T)]^n\quad\forall\,T\in\mathcal{T}_h\Big\}. \tag{3.17}$$

It is well known (see, e.g. [12]) that $H^{\mathbf{u}}_h$ satisfies the following approximation property:

$(\widetilde{\mathrm{AP}}^{\mathbf{u}}_h)$ *For each $s\in[0,k+1]$ and for each $\mathbf{v}\in[H^{1+s}(\Omega)]^n$ there exists $\mathbf{v}_h\in H^{\mathbf{u}}_h$ such that*

$$\|\mathbf{v}-\mathbf{v}_h\|_{1,\Omega}\leq Ch^s\,\|\mathbf{v}\|_{1+s,\Omega}.$$

Hence, the analogue of Theorem 2.4 for the augmented scheme (3.14) is stated next.

Theorem 3.3. *Let* $\boldsymbol{H}_{0,h} := H^{\boldsymbol{\sigma}}_{0,h} \times H^{\mathbf{u}}_h$ *with* $H^{\boldsymbol{\sigma}}_{0,h}$ *and* $H^{\mathbf{u}}_h$ *given by* (2.22) *and* (3.17)*, and let* $(\boldsymbol{\sigma},\mathbf{u}) \in \boldsymbol{H}_0$ *and* $(\boldsymbol{\sigma}_h,\mathbf{u}_h) \in \boldsymbol{H}_{0,h}$ *be the unique solutions of the continuous and discrete augmented formulations* (3.4) *and* (3.14)*, respectively. Assume that* $\boldsymbol{\sigma} \in [H^s(\Omega)]^{n\times n}$, $\mathbf{div}(\boldsymbol{\sigma}) \in [H^s(\Omega)]^n$, *and* $\mathbf{u} \in [H^{1+s}(\Omega)]^n$*, for some* $s \in (0,k+1]$*. Then there exists* $C>0$*, independent of* h*, such that*

$$\|(\boldsymbol{\sigma},\mathbf{u}) - (\boldsymbol{\sigma}_h,\mathbf{u}_h)\|_{\boldsymbol{H}_0} \leq Ch^s \left\{ \|\boldsymbol{\sigma}\|_{s,\Omega} + \|\mathbf{div}(\boldsymbol{\sigma})\|_{s,\Omega} + \|\mathbf{u}\|_{1+s,\Omega} \right\}.$$

Proof. It follows straightforwardly from the Cea estimate (3.15) and the approximation properties $(\mathrm{AP}^{\boldsymbol{\sigma}}_{0,h})$ and $(\widetilde{\mathrm{AP}}^{\mathbf{u}}_h)$. □

4 Numerical results

In this section we present four numerical examples in $\mathbb{R}^3$ illustrating the performance of the mixed finite element schemes (2.18) and (3.14). For examples in $\mathbb{R}^2$ we refer to [20] and [14]. In all the computations we consider the specific finite element subspaces $H^{\boldsymbol{\sigma}}_{0,h}$, Q_h, and $H^{\mathbf{u}}_h$ given by (2.22) and (3.17) with $k=0$. In addition, similarly as in [17] and [14], the zero integral mean condition for tensors in the space $H^{\boldsymbol{\sigma}}_{0,h}$ is imposed in both discrete schemes via a real Lagrange multiplier. Furthermore, as already mentioned in Section 3, the vector of parameters employed for the implementation of each one of the augmented schemes (3.14) is given by $(\kappa_1,\kappa_2,\kappa_3) = (\mu,\frac{1}{2\mu},\mu)$. To this respect, we remark that, though we do not present the corresponding tables here, the same results (up to the first 6 and 7 digits) are obtained with other sets of feasible parameters, which suggests the robustness of (3.14) with respect to the vector $(\kappa_1,\kappa_2,\kappa_3)$.

In what follows, N stands for the total number of degrees of freedom (unknowns) of (2.18) and (3.14), which can be proved (see [19, Section 4] for details) to behave asymptotically as 9 and 6.5 times, respectively, the number of tetrahedrons of each triangulation. Also, the individual and total errors are given by

$$e(\boldsymbol{\sigma}) := \|\boldsymbol{\sigma}-\boldsymbol{\sigma}_h\|_{\mathbf{div},\Omega}, \quad e(p) := \|p-p_h\|_{0,\Omega}, \quad e(\mathbf{u}) := \|\mathbf{u}-\mathbf{u}_h\|_{0,\Omega},$$

$$e_0(\boldsymbol{\sigma}) := \|\boldsymbol{\sigma}-\boldsymbol{\sigma}_h\|_{0,\Omega}, \quad \text{and} \quad e(\boldsymbol{\sigma},\mathbf{u}) := \left\{(e(\boldsymbol{\sigma}))^2 + (e(\mathbf{u}))^2\right\}^{1/2},$$

where the approximate pressure p_h is computed though the post processing formula suggested by the identity (2.1), that is $p_h = \dfrac{1}{3}\mathrm{tr}(\boldsymbol{\sigma}_h)$. In addition, we define the experimental rates of convergence

$$r(\boldsymbol{\sigma}) := \frac{\log(e(\boldsymbol{\sigma})/e'(\boldsymbol{\sigma}))}{\log(h/h')}, \quad r(p) := \frac{\log(e(p)/e'(p))}{\log(h/h')}, \quad r(\mathbf{u}) := \frac{\log(e(\mathbf{u})/e'(\mathbf{u}))}{\log(h/h')},$$

$$r_0(\boldsymbol{\sigma}) := \frac{\log(e_0(\boldsymbol{\sigma})/e'_0(\boldsymbol{\sigma}))}{\log(h/h')}, \quad \text{and} \quad r(\boldsymbol{\sigma},\mathbf{u}) := \frac{\log(e(\boldsymbol{\sigma},\mathbf{u})/e'(\boldsymbol{\sigma},\mathbf{u}))}{\log(h/h')},$$

where e and e' denote the corresponding errors at two consecutive triangulations with mesh sizes h and h', respectively.

The examples to be considered in this section are described next. We take the kinematic viscosity $\mu = 1$ in Examples 1, 2, and 3, and $\mu = 1/2$ in Example 4. Example 1 is employed to illustrate the performance of the mixed finite element schemes when applied to a typical academic problem. Then, Examples 2 and 3 deal with two more realistic situations in fluid mechanics. Finally, in Example 4 we consider the standard test case given by a driven cavity, and compare the results provided by our methods with those obtained by the numerical techniques proposed in [26], [27], and [28], which are based on a velocity-vorticity formulation.

In Example 1 we consider the L-shaped domain $\Omega :=]0,1[^3 - \{[1/2,1]\times[0,1]\times[1/2,1]\}$, and choose the data $\mathbf{f}$ and $\mathbf{g}$ so that the exact solution is given by

$$\mathbf{u}(\mathbf{x}) = \frac{\mathtt{r}^{5/3}}{2}\begin{pmatrix} 2(x_3-0.5)(x_2+0.5) \\ (0.5-x_1)(x_3-0.5) \\ (0.5-x_1)(x_2+0.5) \end{pmatrix},$$

$$p(\mathbf{x}) = \frac{1}{x_3-1.1} - p_0,$$

with $\mathtt{r} = \{(x_1-0.6)^2+(x_2+0.6)^2+(x_3-0.6)^2\}^{1/2}$, for all $\mathbf{x} := (x_1,x_2,x_3)^{\mathtt{t}} \in \Omega$, where $p_0 \in \mathbb{R}$ is such that $\int_\Omega p = 0$.

In Example 2 we consider a 90 degrees elbow duct $\Omega := \Omega_1 \cup \Omega_2 \cup \Omega_3$, where

$$\Omega_1 := \left\{(x_1,x_2,x_3)^{\mathtt{t}} \in \mathbb{R}^3 : \quad x_1^2 + x_2^2 < 1, \quad 0 < x_3 \leq 1\right\},$$

$$\Omega_2 := \left\{(x_1,x_2,x_3)^{\mathtt{t}} \in \mathbb{R}^3 : \quad x_1^2 + (x_3-2)^2 < 1, \quad 1 \leq x_2 < 2\right\},$$

$$\Omega_3 := \left\{(x_1,x_2,x_3)^{\mathtt{t}} \in \mathbb{R}^3 : \quad \left(1-\sqrt{(x_2-1)^2+(x_3-1)^2}\right)^2 + x_1^2 < 1,\, x_2 \leq 1,\, x_3 \geq 1\right\},$$

and choose the data $\mathbf{f}$ and $\mathbf{g}$ so that the exact solution is given by

$$\mathbf{u}(\mathbf{x}) = \begin{pmatrix} 2\sin^2\left(\frac{\pi x_1}{8}\right)\sin\left(\frac{\pi x_2}{4}\right)\sin\left(\frac{\pi x_3}{4}\right) \\ -\sin^2\left(\frac{\pi x_2}{8}\right)\sin\left(\frac{\pi x_1}{4}\right)\sin\left(\frac{\pi x_3}{4}\right) \\ -\sin^2\left(\frac{\pi x_3}{8}\right)\sin\left(\frac{\pi x_1}{4}\right)\sin\left(\frac{\pi x_2}{4}\right) \end{pmatrix},$$

$$p(\mathbf{x}) = \sin\left(\frac{\pi x_1}{4}\right)\sin\left(\frac{\pi x_2}{4}\right)\sin\left(\frac{\pi x_3}{4}\right) - p_0,$$

for all $\mathbf{x} := (x_1,x_2,x_3)^{\mathtt{t}} \in \Omega$, where $p_0 \in \mathbb{R}$ is such that $\int_\Omega p = 0$.

In Example 3 we consider a diffusor duct $\Omega := \Omega_1 \cup \Omega_2 \cup \Omega_3$, where

$$\Omega_1 := \left\{ (x_1,x_2,x_3)^{\mathtt{t}} \in \mathbb{R}^3 : \quad x_1^2 + x_2^2 < 1, \quad -1 < x_3 \leq 0 \right\},$$

$$\Omega_2 := \left\{ (x_1,x_2,x_3)^{\mathtt{t}} \in \mathbb{R}^3 : \quad x_1^2 + x_2^2 < 0.5, \quad 1 \leq x_3 < 2 \right\},$$

$$\Omega_3 := \left\{ (x_1,x_2,x_3)^{\mathtt{t}} \in \mathbb{R}^3 : \quad x_1^2 + x_2^2 < \left(1 - \frac{x_3}{2}\right)^2, \quad 0 \leq x_3 \leq 1 \right\},$$

and choose the data $\mathbf{f}$ and $\mathbf{g}$ so that the exact solution is given by

$$\mathbf{u}(\mathbf{x}) = \exp(-x_1)\exp\left(\frac{x_3}{2}\right) \begin{pmatrix} \dfrac{1}{2}\sin x_1 \cos x_2 \\ \\ \sin x_2 \left(\sin x_1 - \cos x_1\right) \\ \\ \cos x_2 \left(\cos x_1 - \sin x_1\right) \end{pmatrix},$$

$$p(\mathbf{x}) = \cos x_1 \cos x_2 \exp(-x_3) - p_0.$$

for all $\mathbf{x} := (x_1,x_2,x_3)^{\mathtt{t}} \in \Omega$, where $p_0 \in \mathbb{R}$ is such that $\displaystyle\int_\Omega p = 0$.

In Example 4 we consider the cubic cavity $\Omega :=]0,1[^3$, and take the right hand side $\mathbf{f} = \mathbf{0}$ on Ω and the Dirichlet boundary condition

$$\mathbf{g}(\mathbf{x}) := \begin{cases} (1,0,0)^{\mathtt{t}} & \text{if} \quad 0 \leq x_1 \leq 1, \quad 0 \leq x_2 \leq 1, \quad x_3 = 0, \\ (0,0,0)^{\mathtt{t}} & \text{otherwise.} \end{cases}$$

The numerical results shown below were obtained in a *Pentium Xeon computer with dual processors*, using a MATLAB code. In Tables 1 and 2 we summarize the convergence history of the mixed finite element schemes (2.18) and (3.14), respectively, as applied to Example 1 for sequences of quasi-uniform triangulations of the domain. In addition, the approximate pressure p_h has been computed according to the post processing formula indicated above. We observe here that the experimental rate of convergence of each unknown tends asymptotically to the theoretical rate of convergence $O(h)$ predicted by Theorems 2.4 and 3.3 (when $s = 1$). This fact is also illustrated in Figures 1 and 2, where we display the errors vs. the degrees of freedom N. Finally, in order to emphasize the good performance of our schemes, in Figures 3 to 6 we display four components of the approximate and exact solutions for Example 1.

Next, in Tables 3 to 6 we provide the convergence history of the mixed finite element schemes (2.18) and (3.14), as applied to Examples 2 and 3 for sequences of quasi-uniform triangulations of the respective domains. The approximate pressure p_h is again computed via the post processing formula. We observe now that the experimental rates of convergence also tend asymptotically to the theoretical rate of convergence $O(h)$ predicted by Theorems 2.4 and 3.3 (when $s = 1$), but in a more oscillating way than in Example 1. Actually, these oscillations are more pronounced in Example 2 than in Example 3, which

could be caused by the geometry more complicated of the former. This behaviour can also be seen slightly in Figures 7, 8, 12, and 13, where we show the errors vs. the degrees of freedom N. Furthermore, the augmented scheme (3.14) seems to converge a bit faster than (2.18) in these examples, specially for Example 3 (cf. Tables 5 and 6). Nevertheless, both discrete schemes show very satisfactory performances, which is confirmed by Figures 9 to 11 and Figures 14 to 16, where we display three components of the approximate and exact solutions of each example.

Finally, we utilize Example 4 to compare our schemes with those proposed in [26], [27], and [28], which are all based on a velocity-vorticity formulation and employ meshless BEM, traditional BEM-FEM, and multiquadrics methods, respectively. Actually, since Example 3 in [28], which coincides with our present Example 4, already makes the comparison with the results obtained in the previous papers [26] and [27], we just proceed here to incorporate the numerical results arising from our schemes into the same kind of figures provided in [28]. The correspondence of the figures in this paper and in [28] is as follows

Figure in this paper	17	18	19	20	21	22	23	24	25	26	27	28
Figure in [28]	15	16	17	18	19	20	15	16	17	18	19	20

In particular, Figures 17 to 20 display some components of the approximate solutions obtained with our scheme (2.18). This includes an approximation of the vorticity unknown, denoted by $\boldsymbol{\omega} := (\omega_1,\omega_2,\omega_3)^{\mathrm{t}}$, which is computed via a simple post-processing formula: curl operator applied to the velocity vector. For instance, Figure 18 shows the resulting approximation for ω_1, which confirms the expected symmetry with respect to the x and y directions. In addition, Figures 19 and 20 reveal that the effect of the wall (given by the Dirichlet boundary condition $\mathbf{g}$) makes vorticity distribution more concentrated on the edges of the cavity. Then, Figures 21 and 22 makes an explicit comparison of some velocity profiles resulting from (2.18) and the methods from Tsai et al. (2002) [26], Young et al. (1999) [27], and Young et al. (2004) [28]. We observe there that our results also capture the effect of wall at driven direction similarly as the results from the other papers do. The above analysis is repeated in Figures 23 to 28 for the augmented scheme (3.14), obtaining the same conclusions.

Summarizing, we believe that there is enough support to consider the mixed finite element schemes (2.18) and (3.14) as valid and competitive alternatives to solve the stationary Stokes equations in $\mathbb{R}^3$.

Table 1: EXAMPLE 1, quasi-uniform scheme (2.18)

N	h	$e(\boldsymbol{\sigma})$	$r(\boldsymbol{\sigma})$	$e_0(\boldsymbol{\sigma})$	$r_0(\boldsymbol{\sigma})$	$e(\mathbf{u})$	$r(\mathbf{u})$
391	1/2	5.131E−00	–	1.526E−00	–	1.810E−01	–
2857	1/4	4.679E−00	0.133	1.066E−00	0.517	9.446E−02	0.939
9343	1/6	4.127E−00	0.310	8.260E−01	0.630	6.325E−02	0.989
21793	1/8	3.613E−00	0.462	6.667E−01	0.745	4.742E−02	1.001
42151	1/10	3.180E−00	0.573	5.550E−01	0.822	3.790E−02	1.005
72361	1/12	2.823E−00	0.654	4.732E−01	0.874	3.155E−02	1.005
114367	1/14	2.528E−00	0.716	4.114E−01	0.908	2.702E−02	1.005
170113	1/16	2.283E−00	0.763	3.633E−01	0.932	2.363E−02	1.005
241543	1/18	2.078E−00	0.800	3.248E−01	0.950	2.100E−02	1.004
330601	1/20	1.904E−00	0.829	2.935E−01	0.963	1.889E−02	1.004

N	h	$e(p)$	$r(p)$	$e(\boldsymbol{\sigma},\mathbf{u})$	$r(\boldsymbol{\sigma},\mathbf{u})$
391	1/2	5.114E−01	–	5.135E−00	–
2857	1/4	4.288E−01	0.254	4.680E−00	0.134
9343	1/6	3.481E−01	0.514	4.128E−00	0.310
21793	1/8	2.852E−01	0.693	3.614E−00	0.462
42151	1/10	2.384E−01	0.804	3.180E−00	0.573
72361	1/12	2.033E−01	0.873	2.823E−00	0.654
114367	1/14	1.765E−01	0.918	2.528E−00	0.716
170113	1/16	1.555E−01	0.949	2.283E−00	0.763
241543	1/18	1.387E−01	0.971	2.078E−00	0.800
330601	1/20	1.250E−01	0.986	1.904E−00	0.829

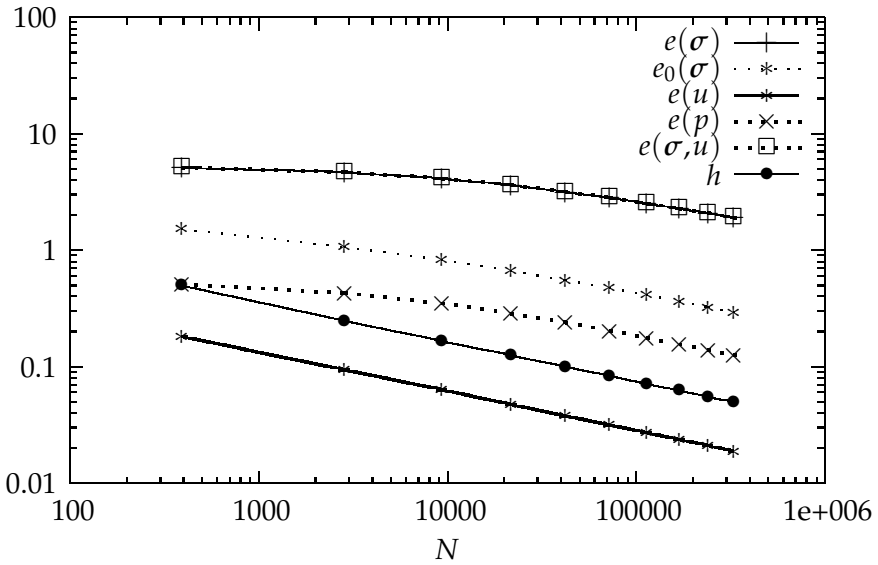

Figure 1: EXAMPLE 1, quasi-uniform scheme (2.18).

Table 2: EXAMPLE 1, quasi-uniform scheme (3.14) with $(\kappa_1,\kappa_2,\kappa_3)=(\mu,\frac{1}{2\mu},\mu)$.

N	h	$e(\boldsymbol{\sigma})$	$r(\boldsymbol{\sigma})$	$e_0(\boldsymbol{\sigma})$	$r_0(\boldsymbol{\sigma})$	$e(\mathbf{u})$	$r(\mathbf{u})$
355	1/2	5.259E−00	–	1.909E−00	–	7.753E−01	–
2308	1/4	4.706E−00	0.160	1.178E−00	0.696	4.651E−01	0.737
7267	1/6	4.134E−00	0.320	8.594E−01	0.779	3.213E−01	0.912
16636	1/8	3.615E−00	0.466	6.747E−01	0.841	2.432E−01	0.968
31819	1/10	3.180E−00	0.575	5.540E−01	0.883	1.950E−01	0.991
54220	1/12	2.822E−00	0.655	4.691E−01	0.912	1.624E−01	1.001
85243	1/14	2.527E−00	0.716	4.064E−01	0.932	1.391E−01	1.006
126292	1/16	2.282E−00	0.763	3.581E−01	0.946	1.216E−01	1.008
178771	1/18	2.077E−00	0.800	3.199E−01	0.957	1.079E−01	1.009
244084	1/20	1.903E−00	0.829	2.890E−01	0.966	9.706E−02	1.009
323635	1/22	1.755E−00	0.853	2.634E−01	0.972	8.816E−02	1.009

N	h	$e(p)$	$r(p)$	$e(\boldsymbol{\sigma},\mathbf{u})$	$r(\boldsymbol{\sigma},\mathbf{u})$
355	1/2	7.105E−01	–	5.316E−00	–
2308	1/4	4.796E−01	0.567	4.729E−00	0.169
7267	1/6	3.561E−01	0.734	4.146E−00	0.324
16636	1/8	2.810E−01	0.823	3.623E−00	0.469
31819	1/10	2.310E−01	0.878	3.186E−00	0.576
54220	1/12	1.956E−01	0.914	2.827E−00	0.656
85243	1/14	1.692E−01	0.938	2.531E−00	0.717
126292	1/16	1.489E−01	0.956	2.285E−00	0.764
178771	1/18	1.329E−01	0.969	2.080E−00	0.800
244084	1/20	1.199E−01	0.979	1.906E−00	0.830
323635	1/22	1.091E−01	0.986	1.757E−00	0.853

Table 3: EXAMPLE 2, quasi-uniform scheme (2.18).

N	h	$e(\boldsymbol{\sigma})$	$r(\boldsymbol{\sigma})$	$e(\mathbf{u})$	$r(\mathbf{u})$	$e(p)$	$r(p)$	$e(\boldsymbol{\sigma},\mathbf{u})$	$r(\boldsymbol{\sigma},\mathbf{u})$
7318	1.000	6.308E−01	–	8.820E−02	–	1.894E−01	–	6.370E−01	–
20767	0.642	4.688E−01	0.670	6.657E−02	0.636	1.402E−01	0.679	4.735E−01	0.670
28945	0.536	4.082E−01	0.765	5.953E−02	0.617	1.213E−01	0.799	4.125E−01	0.762
51703	0.468	3.357E−01	1.436	4.902E−02	1.427	9.773E−02	1.588	3.393E−01	1.436
79921	0.414	2.897E−01	1.206	4.241E−02	1.185	8.276E−02	1.360	2.928E−01	1.206
110248	0.352	2.575E−01	0.726	3.739E−02	0.777	7.301E−02	0.774	2.602E−01	0.727
156391	0.323	2.288E−01	1.358	3.352E−02	1.255	6.442E−02	1.437	2.313E−01	1.355
208492	0.301	2.088E−01	1.321	3.061E−02	1.310	5.824E−02	1.451	2.110E−01	1.320
286951	0.264	1.895E−01	0.737	2.788E−02	0.709	5.260E−02	0.774	1.915E−01	0.736

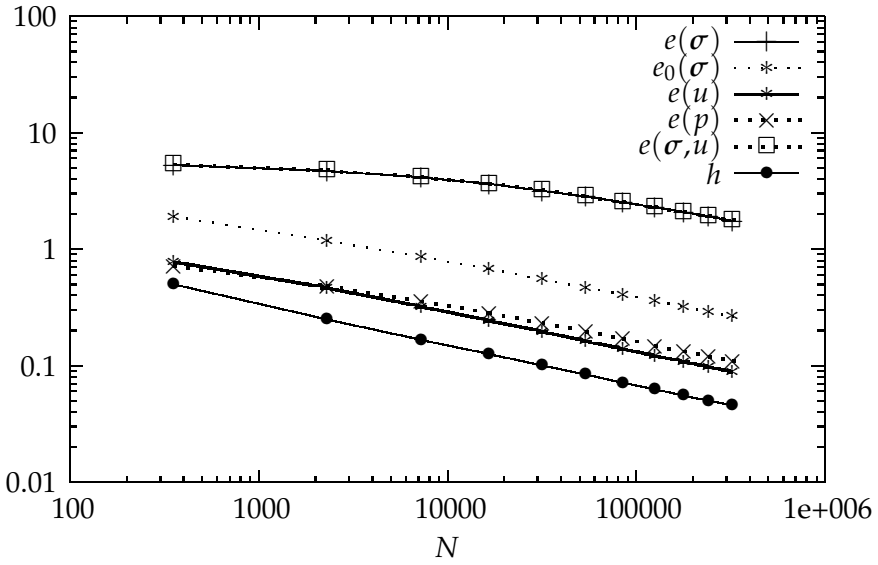

Figure 2: EXAMPLE 1, quasi-uniform scheme (3.14).

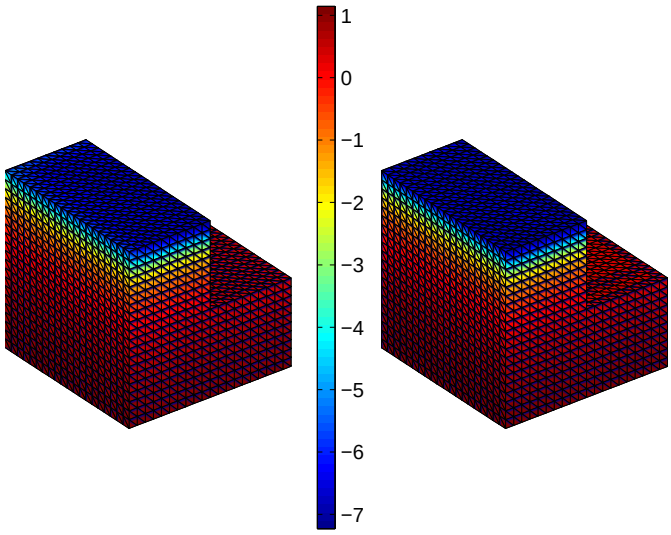

Figure 3: EXAMPLE 1, approximate (left) and exact p for quasi-uniform scheme (3.14) with $h=1/10$.

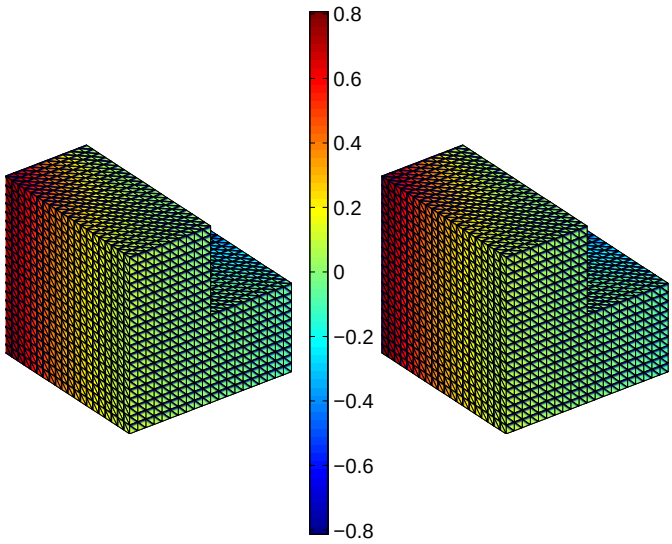

Figure 4: EXAMPLE 1, approximate (left) and exact u_3 for quasi-uniform scheme (3.14) with $h=1/10$.

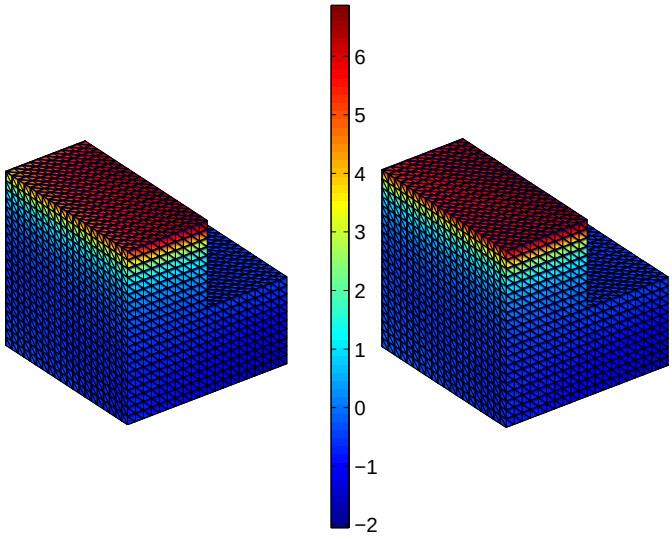

Figure 5: EXAMPLE 1, approximate (left) and exact σ_{11} for quasi-uniform scheme (3.14) with $h=1/10$.

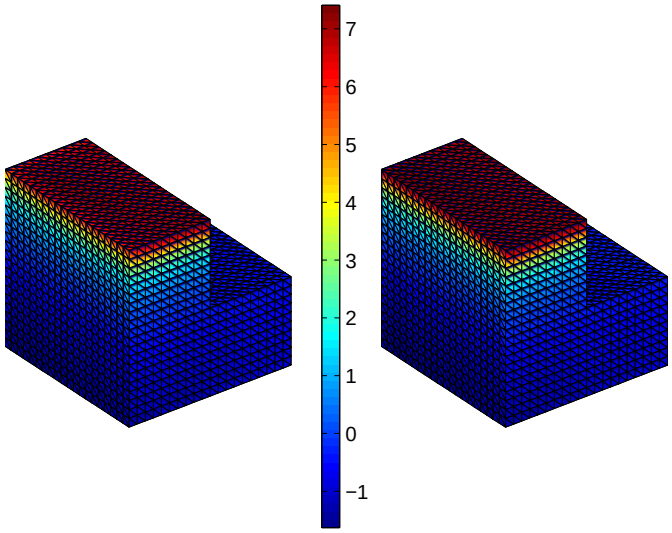

Figure 6: EXAMPLE 1, approximate (left) and exact σ_{33} for quasi-uniform scheme (3.14) with $h=1/10$.

Table 4: EXAMPLE 2, quasi-uniform scheme (3.14) with $(\kappa_1,\kappa_2,\kappa_3)=(\mu,\frac{1}{2\mu},\mu)$.

N	h	$e(\sigma)$	$r(\sigma)$	$e(\mathbf{u})$	$r(\mathbf{u})$	$e(p)$	$r(p)$	$e(\sigma,\mathbf{u})$	$r(\sigma,\mathbf{u})$
5602	1.000	6.345E−01	–	2.917E−01	–	1.484E−01	–	6.983E−01	–
15625	0.642	4.651E−01	0.701	2.147E−01	0.693	1.093E−01	0.692	5.123E−01	0.700
21745	0.536	4.021E−01	0.805	1.859E−01	0.795	9.127E−02	0.994	4.430E−01	0.803
38479	0.468	3.318E−01	1.411	1.540E−01	1.382	7.586E−02	1.358	3.658E−01	1.406
59137	0.414	2.875E−01	1.173	1.342E−01	1.130	6.507E−02	1.255	3.172E−01	1.166
81538	0.352	2.560E−01	0.715	1.210E−01	0.640	5.788E−02	0.723	2.832E−01	0.701
115348	0.323	2.278E−01	1.343	1.073E−01	1.374	5.165E−02	1.307	2.518E−01	1.348
153271	0.301	2.078E−01	1.318	9.753E−02	1.376	4.690E−02	1.387	2.296E−01	1.328
210343	0.264	1.889E−01	0.725	8.950E−02	0.653	4.245E−02	0.758	2.091E−01	0.712
270109	0.246	1.726E−01	1.279	8.192E−02	1.250	3.869E−02	1.311	1.910E−01	1.274

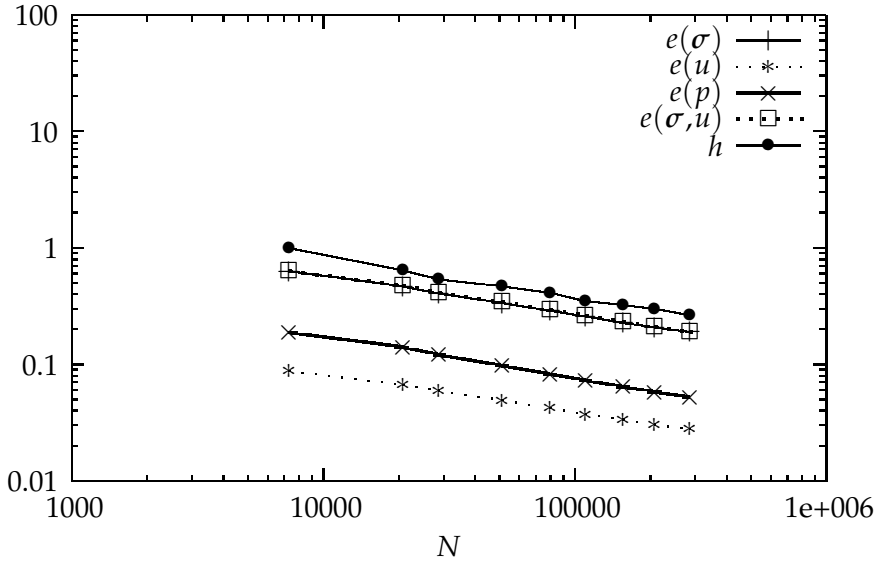

Figure 7: EXAMPLE 2, quasi-uniform scheme (2.18).

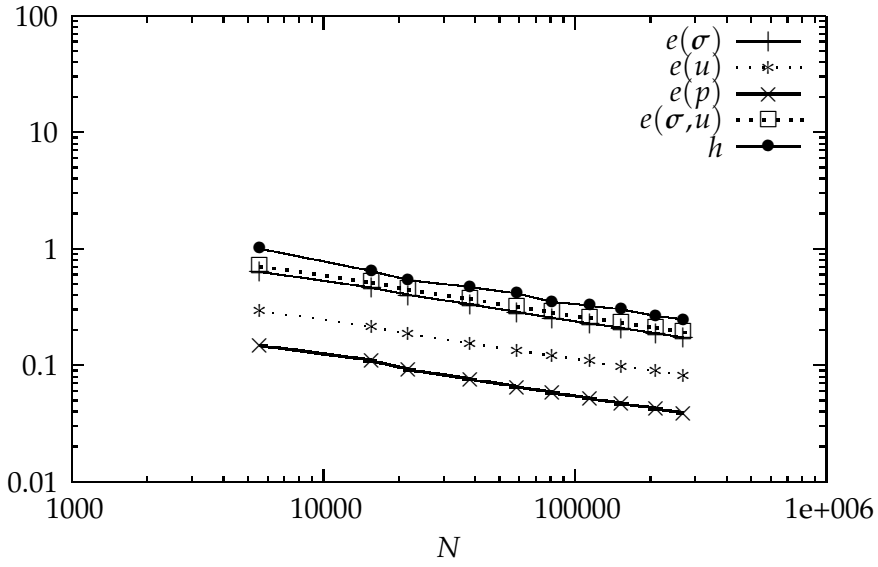

Figure 8: EXAMPLE 2, quasi-uniform scheme (3.14).

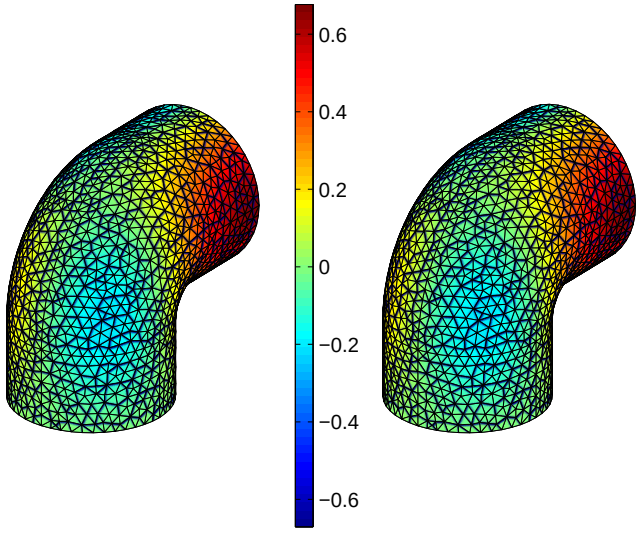

Figure 9: EXAMPLE 2, approximate (left) and exact p for quasi-uniform scheme (3.14) with $h=0.246$.

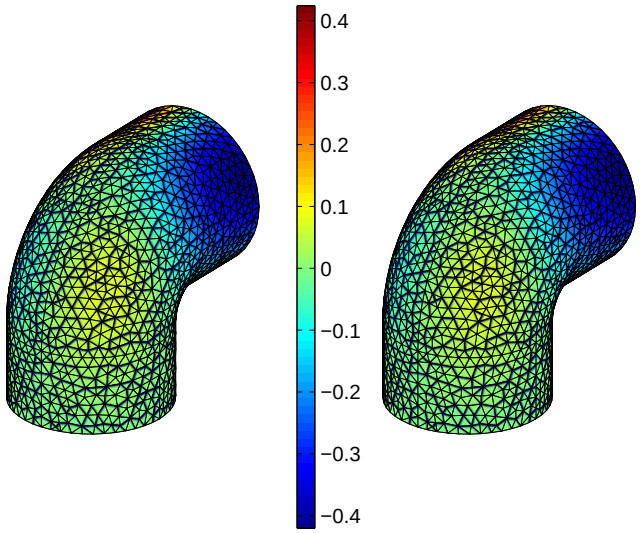

Figure 10: EXAMPLE 2, approximate (left) and exact u_3 for quasi-uniform scheme (3.14) with $h=0.246$.

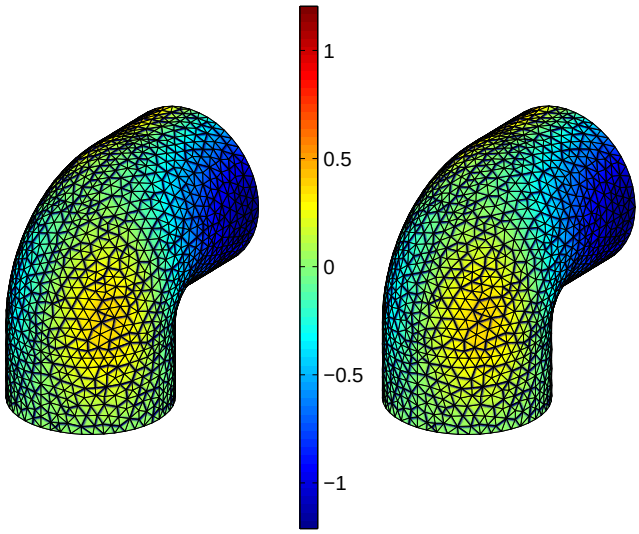

Figure 11: EXAMPLE 2, approximate (left) and exact σ_{33} for quasi-uniform scheme (3.14) with $h=0.246$.

Table 5: EXAMPLE 3, quasi-uniform scheme (2.18).

N	h	$e(\boldsymbol{\sigma})$	$r(\boldsymbol{\sigma})$	$e(\mathbf{u})$	$r(\mathbf{u})$	$e(p)$	$r(p)$	$e(\boldsymbol{\sigma},\mathbf{u})$	$r(\boldsymbol{\sigma},\mathbf{u})$
5125	1.000	3.593E−00	–	6.511E−01	–	9.342E−01	–	3.652E−00	–
16168	0.613	2.137E−00	1.061	4.033E−01	0.978	5.367E−01	1.132	2.175E−00	1.059
22165	0.601	2.032E−00	2.547	3.887E−01	1.866	5.141E−01	2.180	2.069E−00	2.524
33367	0.494	1.692E−00	0.937	3.224E−01	0.958	4.290E−01	0.927	1.723E−00	0.938
60892	0.371	1.383E−00	0.704	2.662E−01	0.669	3.375E−01	0.838	1.409E−00	0.703
68290	0.361	1.331E−00	1.380	2.562E−01	1.369	3.168E−01	2.269	1.355E−00	1.379
126337	0.303	1.081E−00	1.200	2.079E−01	1.202	2.557E−01	1.233	1.100E−00	1.200
201415	0.256	9.209E−01	0.933	1.779E−01	0.910	2.156E−01	0.994	9.379E−01	0.932
266860	0.233	8.355E−01	1.073	1.618E−01	1.041	1.929E−01	1.228	8.510E−01	1.072
289885	0.225	8.086E−01	0.890	1.561E−01	0.977	1.891E−01	0.532	8.235E−01	0.893

Table 6: EXAMPLE 3, quasi-uniform scheme (3.14) with $(\kappa_1,\kappa_2,\kappa_3)=(\mu,\frac{1}{2\mu},\mu)$.

N	h	$e(\boldsymbol{\sigma})$	$r(\boldsymbol{\sigma})$	$e(\mathbf{u})$	$r(\mathbf{u})$	$e(p)$	$r(p)$	$e(\boldsymbol{\sigma},\mathbf{u})$	$r(\boldsymbol{\sigma},\mathbf{u})$
3943	1.000	3.672E−00	–	1.777E−00	–	5.744E−01	–	4.080E−00	–
12196	0.613	2.145E−00	1.098	1.106E−00	0.968	3.004E−01	1.324	2.414E−00	1.072
16810	0.601	2.050E−00	2.312	1.055E−00	2.404	2.834E−01	2.964	2.305E−00	2.331
25018	0.494	1.682E−00	1.011	8.721E−01	0.975	2.231E−01	1.225	1.895E−00	1.004
45469	0.371	1.376E−00	0.702	7.235E−01	0.653	1.792E−01	0.766	1.555E−00	0.692
66199	0.349	1.245E−00	1.603	6.348E−01	2.102	1.636E−01	1.460	1.398E−00	1.709
93679	0.303	1.071E−00	1.081	5.620E−01	0.872	1.344E−01	1.412	1.210E−00	1.037
149026	0.256	9.120E−01	0.937	4.828E−01	0.885	1.143E−01	0.944	1.032E−00	0.926
197092	0.233	8.275E−01	1.072	4.381E−01	1.070	1.019E−01	1.264	9.363E−01	1.072
214078	0.225	8.003E−01	0.909	4.241E−01	0.887	1.003E−01	0.428	9.057E−01	0.904
264484	0.215	7.433E−01	1.644	3.913E−01	1.792	9.288E−02	1.714	8.400E−01	1.676
328606	0.201	6.902E−01	1.088	3.658E−01	0.986	8.551E−02	1.212	7.811E−01	1.065

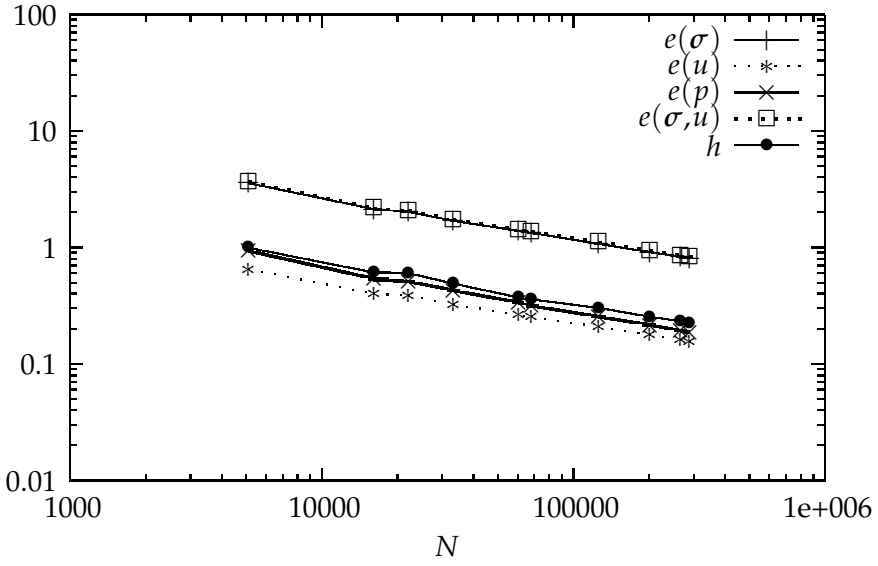

Figure 12: EXAMPLE 3, quasi-uniform scheme (2.18).

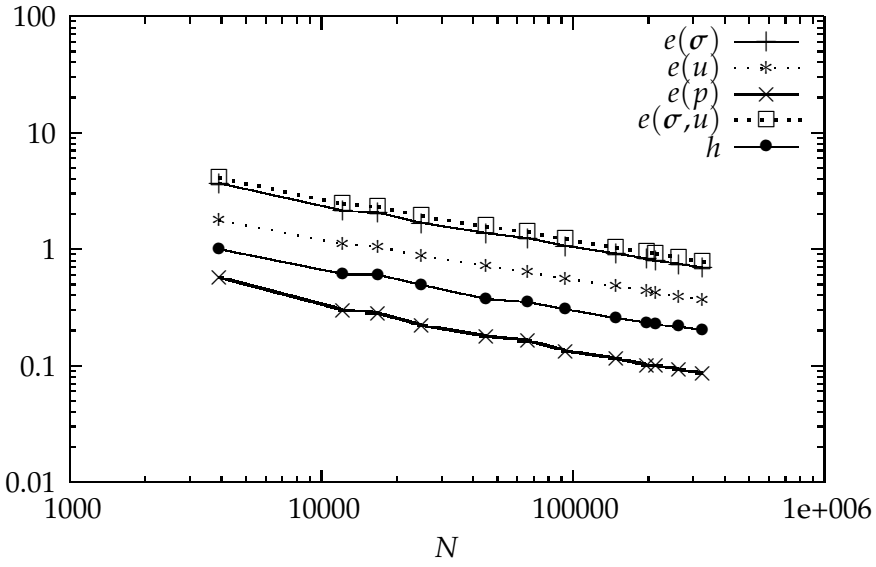

Figure 13: EXAMPLE 3, quasi-uniform scheme (3.14).

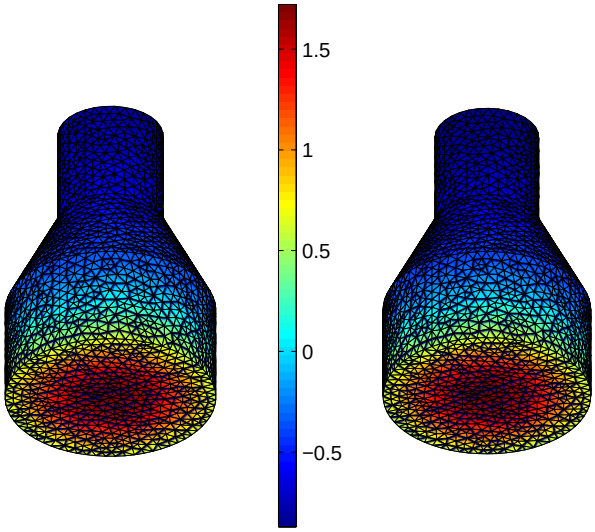

Figure 14: EXAMPLE 3, approximate (left) and exact p for quasi-uniform scheme (3.14) with $h = 0.201$.

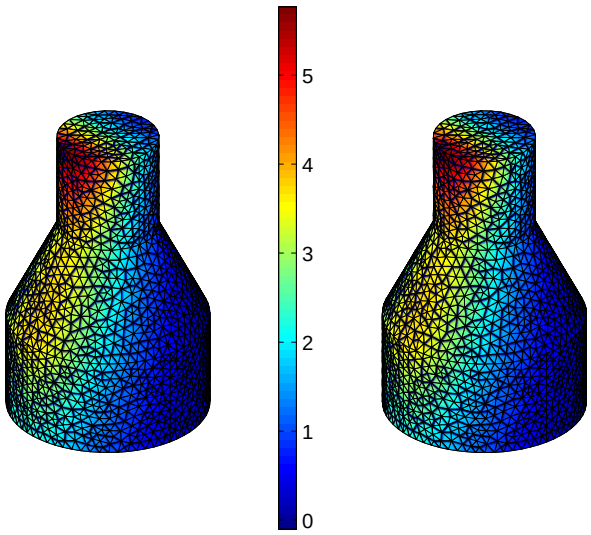

Figure 15: EXAMPLE 3, approximate (left) and exact u_3 for quasi-uniform scheme (3.14) with $h = 0.201$.

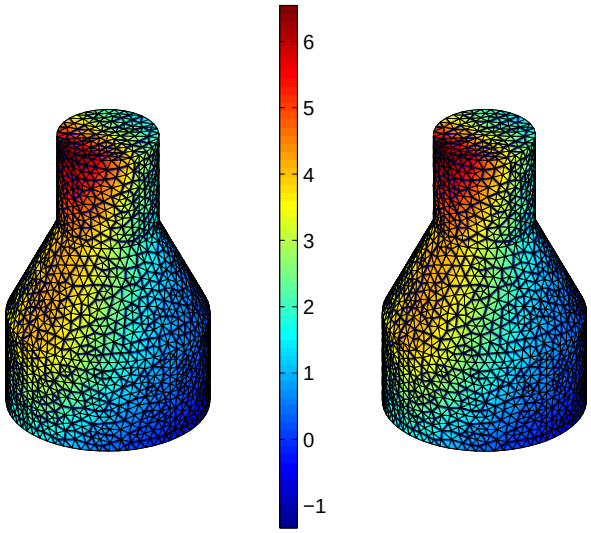

Figure 16: EXAMPLE 3, approximate (left) and exact σ_{33} for quasi-uniform scheme (3.14) with $h = 0.201$.

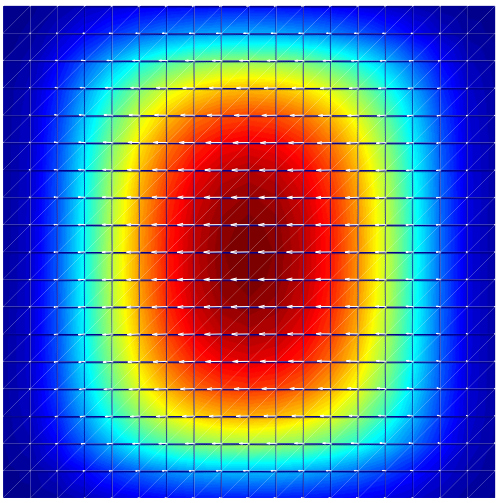

Figure 17: EXAMPLE 4, velocity vectors in $x-y$ plane at $z=0.5$ for quasi-uniform scheme (2.18) with $h=1/18$.

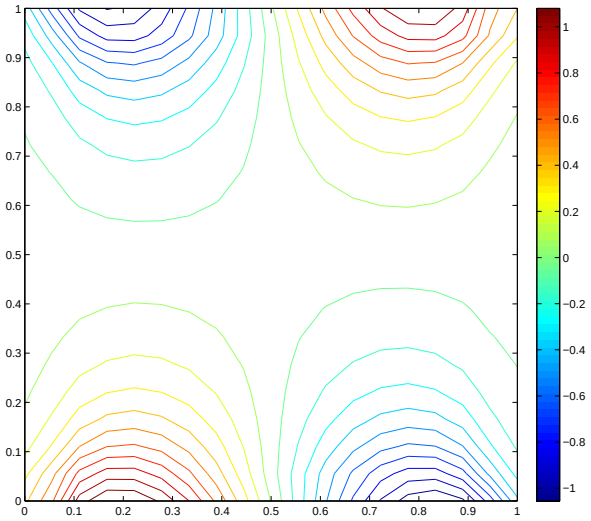

Figure 18: EXAMPLE 4, ω_1 in $x-y$ plane at $z=0.5$ for quasi-uniform scheme (2.18) with $h=1/18$.

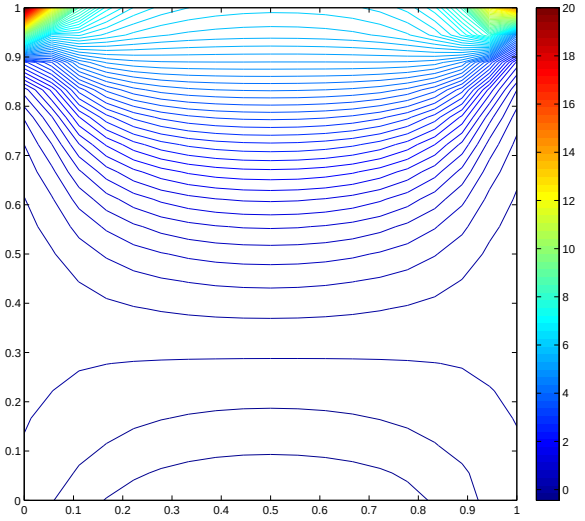

Figure 19: EXAMPLE 4, ω_2 in $y-z$ plane at $x=0.5$ for quasi-uniform scheme (2.18) with $h=1/18$.

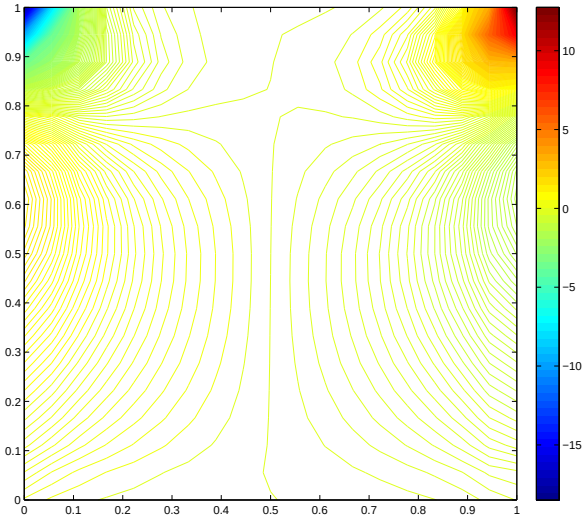

Figure 20: EXAMPLE 4, ω_1 in $y-z$ plane at $x=0.5$ for quasi-uniform scheme (2.18) with $h=1/18$.

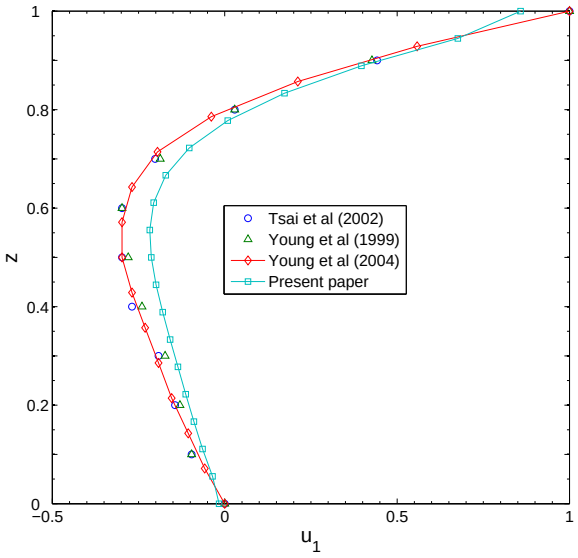

Figure 21: EXAMPLE 4, u_1 along z at $(x,y)=(0.5,0.5)$ for quasi-uniform scheme (2.18) with $h=1/18$.

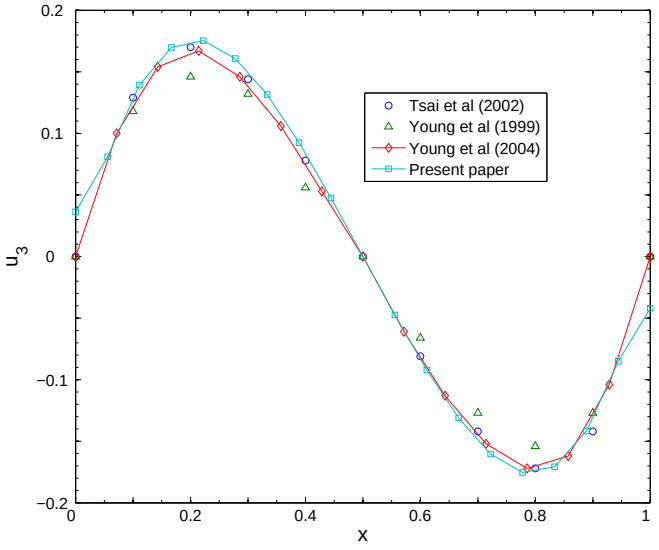

Figure 22: EXAMPLE 4, u_3 along x at $(y,z)=(0.5,0.5)$ for quasi-uniform scheme (2.18) with $h=1/18$.

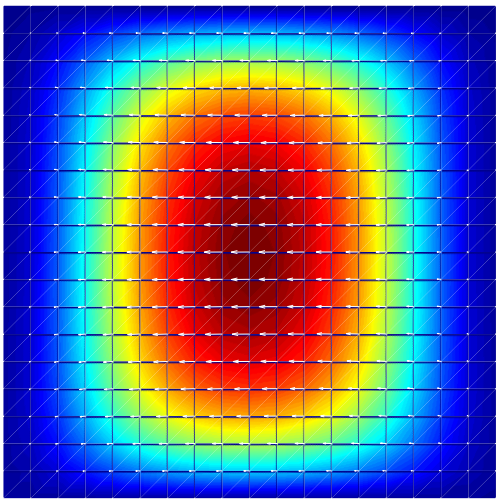

Figure 23: EXAMPLE 4, velocity vectors in $x-y$ plane at $z=0.5$ for quasi-uniform scheme (3.14) with $h=1/18$.

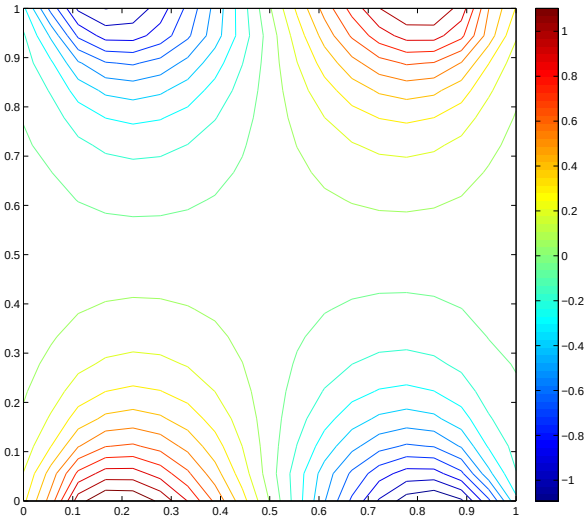

Figure 24: EXAMPLE 4, ω_1 in $x-y$ plane at $z=0.5$ for quasi-uniform scheme (3.14) with $h=1/18$.

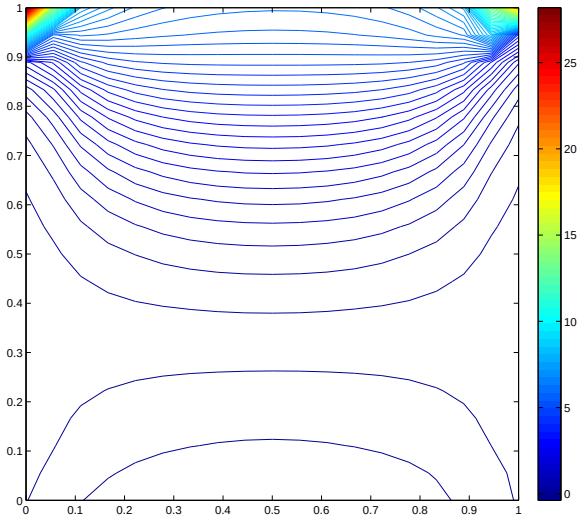

Figure 25: EXAMPLE 4, ω_2 in $y-z$ plane at $x=0.5$ for quasi-uniform scheme (3.14) with $h=1/18$.

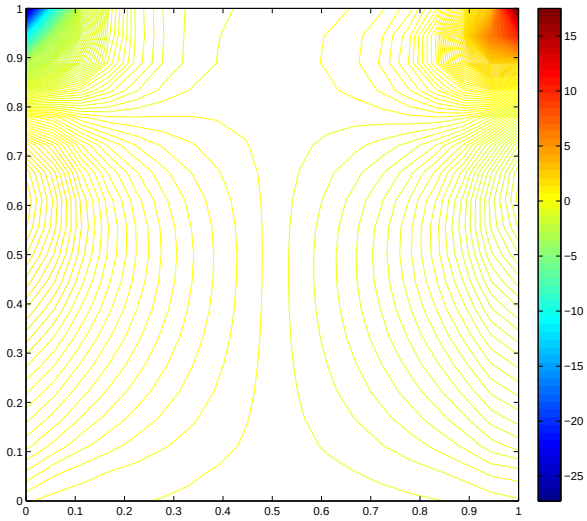

Figure 26: EXAMPLE 4, ω_1 in $y-z$ plane at $x=0.5$ for quasi-uniform scheme (3.14) with $h=1/18$.

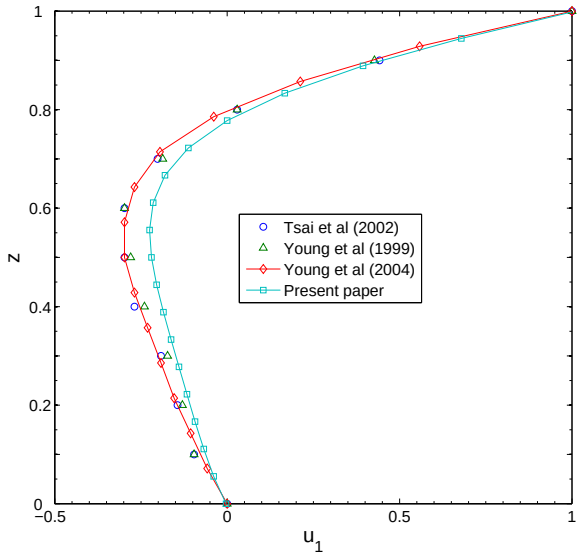

Figure 27: EXAMPLE 4, u_1 along z at $(x,y)=(0.5,0.5)$ for quasi-uniform scheme (3.14) with $h=1/18$.

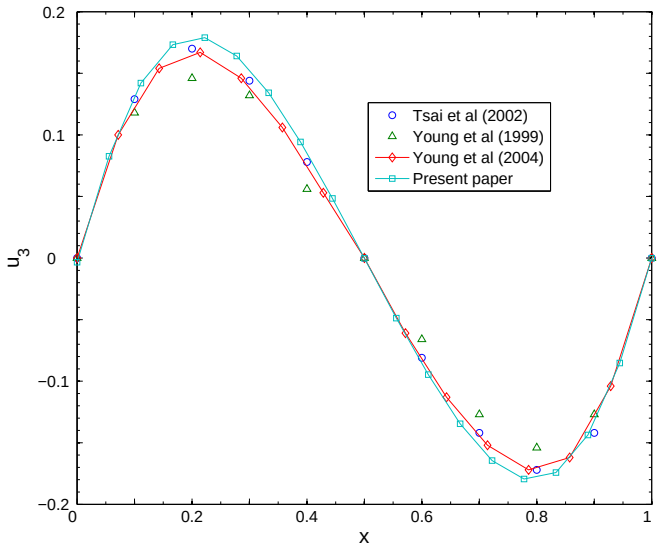

Figure 28: EXAMPLE 4, u_3 along x at $(y,z)=(0.5,0.5)$ for quasi-uniform scheme (3.14) with $h=1/18$.

References

[1] ARNOLD, D.N., BREZZI, F. AND DOUGLAS, J., *PEERS: A new mixed finite element method for plane elasticity*. Japan Journal of Applied Mathematics, vol. 1, 2, pp. 347-367, (1984).

[2] ARNOLD, D.N., DOUGLAS, J. AND GUPTA, CH.P., *A family of higher order mixed finite element methods for plane elasticity*. Numerische Mathematik, vol. 45, pp. 1-22, (1984).

[3] BOCHEV, P.B. AND GUNZBURGER, M.D., *Least-squares methods for the velocity-pressure-stress formulation of the Stokes equations*. Computer Methods in Applied Mechanics and Engineering, vol. 126, 3-4, pp. 267-287, (1995).

[4] BOCHEV, P.B. AND GUNZBURGER, M.D., *Finite element methods of least-squares type*. SIAM Review, vol. 40, 4, pp. 789-837, (1998).

[5] BREZZI, F. AND FORTIN, M., Mixed and Hybrid Finite Element Methods. Springer Verlag, 1991.

[6] CAI, Z., LEE, B. AND WANG, P., *Least-squares methods for incompressible Newtonian fluid flow: Linear stationary problems*. SIAM Journal on Numerical Analysis, vol. 42, 2, pp. 843-859, (2004).

[7] CAI, Z., MANTEUFFEL, T.A. AND MCCORMICK, S.F., *First-order system least squares for the Stokes equations, with application to linear elasticity*. SIAM Journal on Numerical Analysis, vol. 34, 5, pp. 1727-1741, (1997).

[8] CAI, Z. AND STARKE, G., *Least-squares methods for linear elasticity*. SIAM Journal on Numerical Analysis, vol. 42, 2, pp. 826-842, (2004).

[9] CAI, Z., TONG, CH., VASSILEVSKI, P.S. AND WANG, CH., *Mixed finite element methods for incompressible flow: stationary Stokes equations*. Numerical Methods for Partial Differential Equations, vol. 26, 4, pp. 957-978, (2009).

[10] CAI, Z. AND WANG, Y., *A multigrid method for the pseudostress formulation of Stokes problems*. SIAM Journal on Scientific Computing, vol. 29, 5, pp. 2078-2095, (2007).

[11] CHANG, C.L., *A mixed finite element method for the Stokes problem: an acceleration-pressure formulation*. Applied Mathematics and Computation, vol. 36, 2, pp. 135-146, (1990).

[12] CIARLET, P.G., The Finite Element Method for Elliptic Problems. North-Holland, 1978.

[13] FIGUEROA, L., GATICA, G.N. AND HEUER, N., *A priori and a posteriori error analysis of an augmented mixed finite element method for incompressible fluid flows*. Computer Methods in Applied Mechanics and Engineering, vol. 198, 2, pp. 280-291, (2008).

[14] FIGUEROA, L., GATICA, G.N. AND MÁRQUEZ, A., *Augmented mixed finite element methods for the stationary Stokes Equations*. SIAM Journal on Scientific Computing, vol. 31, 2, pp. 1082-1119, (2008).

[15] FRAEJIS DE VEUBEKE, B.M., *Stress function approach*. In: Proceedings of the World Congress on Finite Element Methods in Structural Mechanics, vol. 1, Bournemouth, Dorset, England (October 12-17, 1975), J.1 - J.51.

[16] GATICA, G.N., *An augmented mixed finite element method for linear elasticity with non-homogeneous Dirichlet conditions*. Electronic Transactions on Numerical Analysis, vol. 26, pp. 421-438, (2007).

[17] GATICA, G.N., *Analysis of a new augmented mixed finite element method for linear elasticity allowing* $\mathbb{RT}_0 - \mathbb{P}_1 - \mathbb{P}_0$ *approximations*. ESAIM Mathematical Modelling and Numerical Analysis, vol. 40, 1, pp. 1-28, (2006).

[18] GATICA, G.N., GONZÁLEZ, M. AND MEDDAHI, S., *A low-order mixed finite element method for a class of quasi-Newtonian Stokes flows*. I: *A priori error analysis*. Computer Methods in Applied Mechanics and Engineering, vol. 193, 9-11, pp. 881-892, (2004).

[19] GATICA, G.N., MÁRQUEZ, A. AND MEDDAHI, S., *An augmented mixed finite element method for 3D linear elasticity problems*. Journal of Computational and Applied Mathematics, vol. 231, 2, pp. 526-540, (2009).

[20] GATICA, G.N., MÁRQUEZ, A. AND SÁNCHEZ, M.A., *Analysis of a velocity-pressure-pseudostress formulation for incompressible flow*. Computer Methods in Applied Mechanics and Engineering, vol. 199, 17-20, pp. 1064-1079, (2010).

[21] GATICA, G.N., MÁRQUEZ, A. AND SÁNCHEZ, M.A., *A priori and a posteriori error analyses of a velocity-pseudostress formulation for a class of quasi-Newtonian Stokes flows*. Computer Methods in Applied Mechanics and Engineering, vol. 200, 17-20, pp. 1619-1636, (2011).

[22] GIRAULT, V. AND RAVIART, P.-A., Finite Element Methods for Navier-Stokes Equations. Theory and Algorithms. Springer Series in Computational Mathematics, vol. 5, Springer-Verlag, 1986.

[23] HIPTMAIR, R., *Finite elements in computational electromagnetism*. Acta Numerica, vol. 11, pp. 237-339, (2002).

[24] HOWELL, J.S., *Dual-mixed finite element approximation of Stokes and nonlinear Stokes problems using trace-free velocity gradients*. Journal of Computational and Applied Mathematics, vol. 231, 2, pp. 780-792, (2009).

[25] ROBERTS, J.E. AND THOMAS, J.M., Mixed and Hybrid Methods. In: Handbook of Numerical Analysis, edited by P.G. Ciarlet and J.L. Lions, vol. II, Finite Element Methods (Part 1), 1991, North-Holland, Amsterdam.

[26] TSAI, C.C. YOUNG, D.L. CHENG, A.H.-D., *Meshless BEM for three-dimensional Stokes flows*. Computer Modeling in Engineering and Sciences, vol. 3, 1, pp. 117-128, (2002).

[27] YOUNG, D.L., LIU, Y.H., ELDHO, T.I., *Three-dimensional Stokes flow solution using combined boundary element and finite element methods*. Chinese Journal of Mechanics, vol. 15, pp. 169-176, (1999).

[28] YOUNG, D.L., JANE, S.C., LIN, C.Y., CHIU, C.L., CHEN, K.C., *Solutions of 2D and 3D Stokes laws using multiquadrics method*. Engineering Analysis with Boundary Elements, vol. 28, 10, pp. 1233-1243, (2004).

Centro de Investigación en Ingeniería Matemática (CI^{2}MA)

PRE-PUBLICACIONES 2010 - 2011

2010-17 Rommel Bustinza, Francisco J. Sayas: *Error estimates for an LDG method applied to Signorini type problems*

2010-18 Fabián Flores-Bazán, Fernando Flores-Bazán, Cristian Vera: *A complete characterization of strong duality in nonconvex optimization with a single constraint*

2010-19 Gabriel N. Gatica, Ricardo Oyarzúa, Francisco J. Sayas: *A twofold saddle point approach for the coupling of fluid flow with nonlinear porous media flow*

2010-20 Gabriel N. Gatica, Antonio Marquez, Manuel A. Sanchez: *A priori and a posteriori error analyses of a velocity-pseudostress formulation for a class of quasi-Newtonian Stokes flows*

2010-21 Raimund Bürger, Rosa Donat, Pep Mulet, Carlos A. Vega: *On the implementation of WENO schemes for a class of polydisperse sedimentation models*

2010-22 Fernando Betancourt, Raimund Bürger, Kenneth H. KARLSEN, Elmer M. Tory: *On nonlocal conservation laws modeling sedimentation*

2010-23 Ricardo Durán, Rodolfo Rodríguez, Frank Sanhueza: *A finite element method for stiffened plates*

2010-24 Fabián Flores-Bazán, Felipe Lara: *Inner and outer estimates for solution sets and their asymptotic cones in vector optimization*

2010-25 Tomás Barrios, Rommel Bustinza: *An augmented discontinuous Galerkin method for stationary Stokes problem*

2011-01 Alfredo Bermúdez, Rafael Muñoz-Sola, Carlos Reales, Rodolfo Rodríguez, Pilar Salgado: *A proof of the Reynolds transport theorem in the space $W^{1,1}(Q)$. Extension to cylindrical coordinates*

2011-02 Raimund Bürger, Ricardo Ruiz-Baier, Kai Schneider, Hector Torres: *A multiresolution method for the simulation of sedimentation in inclined channels*

2011-03 Gabriel N. Gatica, Antonio Marquez, Manuel A. Sanchez: *Pseudostress-based mixed finite element methods for the Stokes problem in R^n with Dirichlet boundary conditions. I: A priori error analysis*

Para obtener copias de las Pre-Publicaciones, escribir o llamar a: Director, Centro de Investigación en Ingeniería Matemática, Universidad de Concepción, Casilla 160-C, Concepción, Chile, Tel.: 41-2661324, o bien, visitar la página web del centro: `http://www.ci2ma.udec.cl`







Centro de Investigación en
Ingeniería Matemática (CI²MA)
Universidad de Concepción

Casilla 160-C, Concepción, Chile
Tel.: 56-41-2661324/2661554/2661316
http://www.ci2ma.udec.cl